Mobile and Compact NMR

Bernhard Blümich

Contents

Abstract

NMR with mobile and compact devices is experiencing considerable growth in recent years in particular since instruments have become available, which are capable not only of measuring NMR relaxation but also images and high-resolution spectra. Based on permanent magnet technology, compact tabletop NMR instruments measure samples of materials and solutions positioned inside the magnet, while compact mobile instruments measure material properties of intact objects and samples nondestructively in the inhomogeneous stray field outside the magnet. Following a brief introduction to NMR with homogeneous and inhomogeneous magnetic fields and to the concepts of permanent center- and stray-field NMR magnets, the evolution of the technology over the past 10 years is reviewed and illustrated with selected applications. Relaxation and diffusion measurements find use in the analysis of foods, biological tissues, polymer materials, porous media, and objects of cultural heritage. Compact imaging

B. Blümich (✉)
Institut für Technische und Makromolekulare Chemie, RWTH Aachen University, Aachen, Germany
e-mail: bluemich@itmc.rwth-aachen.de

G.A. Webb (ed.), *Modern Magnetic Resonance*,
DOI 10.1007/978-3-319-28275-6_75-1

instruments are mainly employed to study crops and plants as well as transport phenomena in chemical engineering and geophysics. Tabletop NMR spectrometers find increasing use in educational institutions and for chemical analysis and reaction monitoring on the workbench and in the fume hood of the synthesis laboratory, and they are being explored as a tool for process control.

Keywords
Mobile NMR • Compact NMR • Spectroscopy • Relaxometry • Diffusometry • Laplace NMR • Magnetic resonance imaging • Reaction monitoring • Depth profiling • Distribution of relaxation times • Stray-field NMR • NMR-MOUSE • Permanent magnets • Food • Biological tissue • Polymers • Porous media • Cultural heritage • Miniaturization • Well logging

Introduction

NMR with mobile and compact devices has gained momentum in recent years [1–5] as instruments have become available commercially, which are capable not only of measuring NMR relaxation but also images and high-resolution spectra [1, 6]. Compact tabletop NMR instruments have originally been developed for food analysis based on NMR relaxation and diffusion parameters [7, 8], and mobile instruments have been designed for inspecting bore holes in oil fields [9]. Early on the NMR well-logging technology [10, 11] was explored for nondestructive testing of materials, in particular of polymer materials and moisture in porous media with compact mobile sensors [4, 12–14]. Both the older-generation compact tabletop instruments (Fig. 1a) and the compact mobile devices for nondestructive testing (Fig. 1b, c) employ permanent magnets that only allow measuring relaxation and diffusion but not high-resolution spectra due to the inhomogeneity of the magnetic

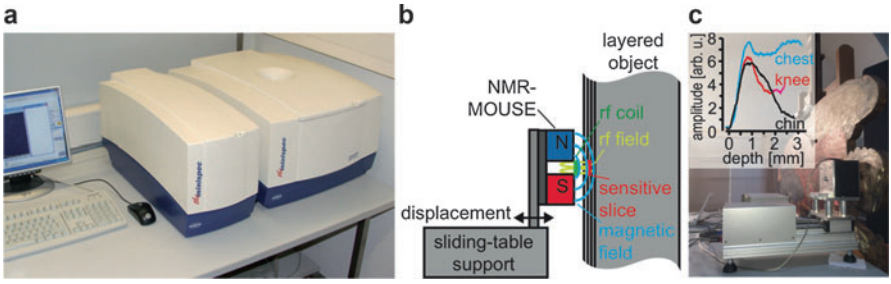

Fig. 1 Compact NMR instruments with inhomogeneous fields for materials testing by Laplace NMR concerning relaxation and diffusion measurements. (**a**) Bruker Minispec. (**b**) Illustration of the NMR-MOUSE for depth profiling. (**c**) The NMR-MOUSE in operation measuring depth profiles through a painted wooden board showing an angel. The *inset* reports the depth profiles of a relaxation-weighted spin density across 3 mm from the painted surface into the board

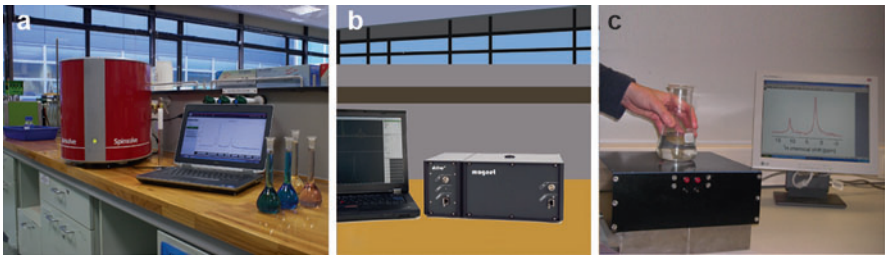

Fig. 2 Magnets for Fourier NMR with approximately homogeneous fields across parts of the sample. (**a**) Tabletop high-resolution NMR spectrometer by Magritek. (**b**) Tabletop tomograph by Pure Devices. (**c**) Prototype of a stray-field magnet capable of measuring chemical-shift-resolved ^{1}H NMR spectra of solutions

field. Once the technology to build permanent magnets with sub-ppm field homogeneity had been developed, this situation has changed considerably (Fig. 2) [3], and the quest today is to develop NMR instruments as small and compact as a cell phone for high-volume markets to be cultivated in the materials testing and health sectors [15–17].

Magnets and Instruments

The degree of field inhomogeneity varies vastly between the different types of compact instruments. Tabletop relaxometers employ magnets constructed with the aim of providing maximum field homogeneity in a field region enclosed by at least three of the six sides of a cuboid (Fig. 3a, b) [18–20], while compact sensors that derive from mobile well-logging tools require a field gradient to collect the NMR signal from a sensitive volume localized outside the magnet (Fig. 3c, d) [21–25]. This is why the latter technology is known also as unilateral NMR (Fig. 1b, c). In the following the two types of magnets are referred to as center-field magnets (Fig. 3a, b) and stray-field magnets (Fig. 3c, d) [26]. Stray-field magnets are simple to construct but usually have field gradients at least one order of magnitude larger than center-field magnets. In fact, for a long time it has been accepted as self-evident, that the chemical shift cannot be resolved in the stray field of a magnet, because the stray field was understood to be highly inhomogeneous [27].

Stray-field NMR for materials testing gained popularity with the appearance of the NMR-MOUSE in 1996 [28]. This simple construction of two magnets placed on an iron yoke (Fig. 3c) [12, 28] collects the NMR signal from an oddly shaped volume located up to a distance typically 5–25 mm away from the magnet surface. The shape of this volume and the associated magnetic field distribution are defined by the arrangement of the magnet blocks, for example, by the size of the gap between them (Fig. 3c, d). Eventually a simple way was found to produce a flat planar slice parallel to the surface, so thin that depth profiles or 1D images could be measured by

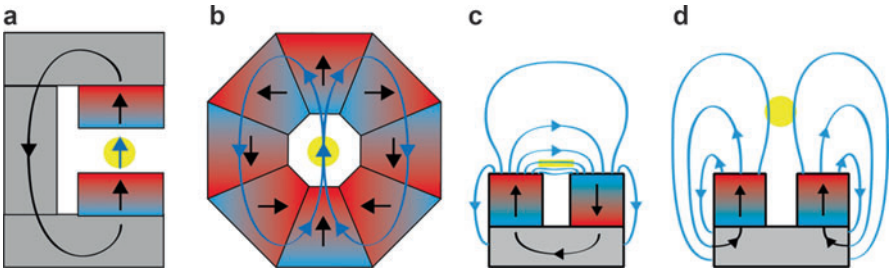

Fig. 3 Types of compact NMR magnets. The sensitive volumes are colored in yellow. (**a**) C-shaped center-field magnet. (**b**) Halbach magnet. (**c**) Stray-field magnet with the field parallel to the magnet surface. (**d**) Stray-field magnet with the field perpendicular to the magnet surface

shifting the sensitive slice through the object with a depth resolution of better than 10 μm (Fig. 1b, c) [29]. By incorporating small and displaceable magnet blocks in the gap of the NMR-MOUSE, it was discovered that the magnetic field could be shimmed to a constant gradient across the volume of a slice up to 2 mm thick and distant from the sensor surface [30] and in a remote-sensitive volume even to homogeneity good enough to acquire chemical-shift-resolved ^{1}H NMR spectra of fluids placed in a beaker on top of the stray-field magnet (Fig. 2c) [27].

In consequence also different designs of permanent center-field magnets were explored for their use in NMR spectroscopy. One approach is to find the least inhomogeneous volume region for the sample inside a magnet gap much larger than the sample and shim the field there with electrical current shims to spectroscopic homogeneity (Fig. 3a) [31]. Another approach is to shim the field of a Halbach magnet by means of displaceable magnet elements [32]. Halbach magnets are cylinder magnets where the magnetization is transverse to the axis of the borehole and the stray field outside is vanishingly small (Fig. 3b) [33]. The net result of these efforts is that today a range of compact NMR instruments is available commercially from different manufacturers, which is suitable for NMR relaxometry, NMR imaging, and NMR spectroscopy [6].

Measurement Methods

Depending on the degree of magnetic field homogeneity, there are two major types of NMR measuring techniques in use today (Fig. 4) [1, 6, 34]. Both employ radio-frequency (rf) pulses for excitation. If the field is sufficiently homogeneous across the extension of the sample, a free induction decay (FID) can be observed in response to a radio-frequency (rf) pulse (Fig. 4a, c). The Fourier transform of the FID provides the distribution resonance frequencies in the sample (Fig. 4c). In chemical analysis this distribution is known as the NMR spectrum. With magnetic resonance imaging (MRI) the spectrum is acquired in the presence of a linearly varying magnetic field. Given that the resonance frequency is proportional to the field strength, the NMR spectrum in this case reveals the concentration of spins as a function of position along the

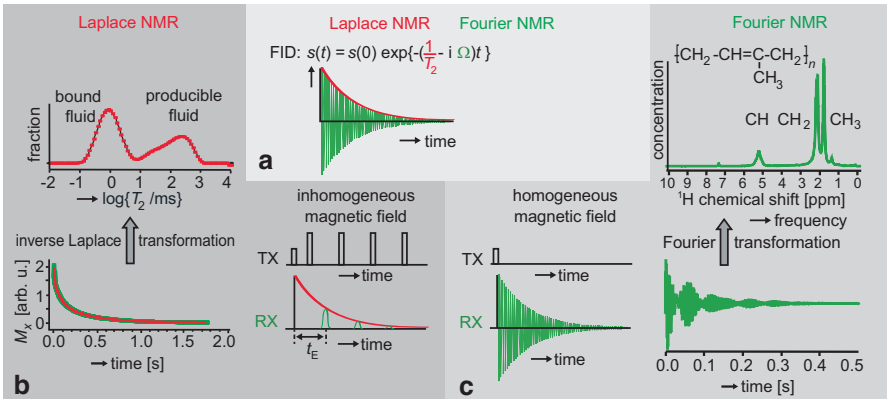

Fig. 4 NMR measurements with pulsed excitation. (**a**) Free induction decay observed in homogeneous magnetic field. The transverse relaxation time is denoted with T_2 and the resonance frequency with Ω. (**b**) Laplace NMR: in inhomogeneous field, only the envelope (*red*) of the FID can be observed stroboscopically with a multi-pulse sequence generating a train of echoes (*right*). Laplace inversion of the echo envelope (*bottom left*) produces a distribution of relaxation times (*top left*) illustrated with signals from water saturating the pores in tuff stone. (**c**) Fourier NMR: in homogeneous field, also the complete FID (*green*) can be observed in response to a single rf impulse. Fourier transform of the FID (*bottom right*) produces a distribution of frequencies, i.e., the NMR spectrum (*top right*) illustrated with signal from a solution of natural rubber. TX stands for transmitter and RX for receiver

gradient direction. Such a spectrum is a projection of the object onto the gradient direction. From many such projections measured in different directions, a spin density image of the object can be reconstructed. In recognition of the Fourier transform as the essential data processing step, NMR spectroscopy and NMR imaging with pulsed excitation are classified as forms of Fourier NMR.

When the magnetic field is so inhomogeneous, that only a particular region of the sample or the object can be excited, an FID can no longer be observed, but the decay envelope of the transverse magnetization can stroboscopically be recalled in NMR echoes generated with two or more rf pulses (Fig. 4b). In this case it is helpful to describe the observed decay envelope by a sum of many exponential functions. Each function decays with a different relaxation rate $1/T_2$, where T_2 is the transverse relaxation time. By algrithms reminiscent of the inverse Laplace transformation applied to the measured decay, the concentrations of all exponential decays in the sum are retrieved as a function of the logarithm of the decay rate $1/T_2$. Similar arguments apply to the signal buildup by longitudinal relaxation with relaxation times T_1 and the signal decay due to translational diffusion with diffusion coefficients D. The inverse Laplace transform applied to an NMR signal decay envelope or the magnetization buildup curve is known as a distribution of relaxation times or diffusion coefficients. The measurement of relaxation times and diffusion coefficients may thus be referred to as Laplace NMR. While Fourier NMR can be conducted only in sufficiently homogeneous magnetic fields, Laplace NMR can be conducted in inhomogeneous as well as homogeneous magnetic fields.

In general, both Laplace and Fourier NMR produce multimodal distributions of NMR parameters with more than one peak (Fig. 4). The maximum number of peaks observable in either type of distribution, however, differs vastly. It is up to about 4 in Laplace NMR and can be more than 100 in Fourier NMR. Nevertheless, the area under a peak can provide the relative concentration of a component signal, for example, of bound or producible fluid in a porous rock (Laplace NMR) or of nuclei in a chemical group of a molecule (Fourier NMR spectroscopy). In an NMR spectrum of a fluid mixture such as crude oil or a body fluid, several peaks may form a sub-spectrum originating from one compound, and the sum of all sub-spectra constitutes the spectrum observed from the fluid with overlapping signals. Signal overlap in 1D distributions can be decreased and the signal assignment facilitated by expanding the distribution into more than one dimension leading to two-dimensional and multidimensional NMR [35, 36]. 2D Fourier NMR, 2D Laplace NMR, and mixed 2D Fourier-Laplace NMR are techniques available today also with compact instruments. In the early days, when NMR experiments were conducted at field strengths similar to those of today's compact instruments, two-dimensional NMR including NMR imaging had not been invented. Then NMR spectra were mostly measured by forced oscillations with slow continuous-wave excitation and hardly with the far more versatile free oscillations employing pulsed excitation, which is exclusively used today in NMR. Yet even then NMR was a method highly appreciated by scientists for chemical analysis [37].

Applications of Mobile and Compact NMR

Mobile and compact NMR instruments are employed in a wide variety of studies. Their use is summarized in books [1, 2, 21] and review articles [3, 6, 13, 22, 24, 38–41]. Representative applications are presented in the following.

Relaxometry and Diffusometry

Relaxometry and diffusometry are known in the NMR community often as low-resolution NMR or time-domain NMR, because mostly instruments are employed with magnetic fields too inhomogeneous to resolve the chemical shift, so that only the buildup and decay of NMR signals by relaxation, diffusion, and related phenomena can be observed. Depending on the type of magnet, tabletop instruments with center-field magnets are used for testing physical properties of material samples, and instruments with stray-field magnets can be carried to the site of the object for nondestructive testing. Stray-field instruments can in principle do the same as center-field instruments. But because their gradients are stronger, the interrogated sample volume is usually smaller, so that for the benefit of precision and short measurement time, the use of center-field instruments is preferred whenever there is a choice.

In either case, the scheme for detecting signal in inhomogeneous fields is the same. An echo of the rapidly decaying FID is generated with a second excitation pulse to recover the signal at the echo time t_E after the first excitation pulse (Fig. 4b, right), and trains of echoes can be generated with a pulse train. The standard pulse train is the CPMG sequence named after Carr, Purcell, Meiboom, and Gill [42, 43]. It has been revisited and optimized for maximum signal gain in stray-field NMR in particular for the oil industry [44–46]. Moreover, phase glitches observed with CPMG-like sequences on many low-field instruments have been tracked to the lack of synchronization of the envelopes to the phase of the rf excitation pulses [47].

Just like the FID, CPMG echo trains are employed for indirect detection of phenomena not directly observable by modulation of the initial state of the spin system at the beginning of the CPMG observation period. This scenario is encountered in measurements of multi-quantum phenomena, longitudinal relaxation, and diffusion and naturally leads to 2D Laplace experiments where the distribution of transverse relaxation times is detected directly and distributions of diffusion coefficients, longitudinal relaxation times, or transverse relaxation times are detected indirectly. The most popular 2D Laplace experiments are T_2-T_2 exchange NMR, T_1-T_2 correlation NMR, and D-T_2 correlation NMR [1, 6, 36, 48]. To encode diffusion, instruments with magnetic field gradients are needed. These are tabletop instruments employing center-field magnets featuring pulsed field gradients (Fig. 1a) and mobile stray-field sensors featuring time-invariant gradients (Fig. 1b).

Food

The development of tabletop NMR relaxometers had started by addressing the needs of the food industry for a reliable method to determine the solid fat content [7, 49]. Today this is still the major application of tabletop NMR followed by droplet sizing of emulsions and liquid typing and quantification in products such as oil in olives [49–56]. The droplet sizing technique has recently been extended to the characterization of double emulsions, where molecular exchange between different compartments of the same phase poses new challenges [57]. With relaxometers, the two liquid phases of an emulsion are distinguished based on their different relaxation times and diffusion coefficients. With the recent availability of tabletop NMR spectrometers with pulsed field gradients, the signals of both components can now be separated based on differences in chemical structure, which usually give rise to large chemical shift differences for immiscible fluids and can be detected with simple pulse sequences [1]. Mobile stray-field sensors, on the other hand, bear promise for inspecting packed food [58–60] and even live animals [61]. For example, a stray-field sensor has been developed for inspecting the quality of meat in life cattle and demonstrated to report clear differences in CPMG decays from fat, lean meat, and marbled rib meat (Fig. 5). Moreover, water and fat content could be determined quantitatively from a bi-exponential analysis of the relaxation curves [61].

Instead of fitting the detected time-domain signal with bi-exponential or other model functions, distributions of relaxation times or diffusion coefficients can be derived by algortithms reminiscent of Laplace inversion [62–64]. With an efficient 2D Laplace inversion algorithm becoming available [65], 2D Laplace NMR has

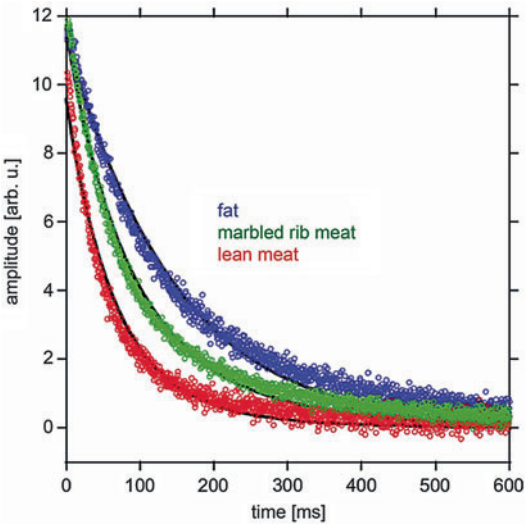

Fig. 5 CPMG decays of meat measured with a stray-field NMR scanner, suggesting that the quality of meat can be discriminated by their relaxation decays even in life cattle (Adapted with permission from [61])

rapidly gained popularity, because ambiguity from signal overlap in 1D distributions can often be resolved in 2D distributions [36]. For example, soft and hard cheese can well be discriminated in T_1-T_2 correlation maps (Fig. 6, left), and the signals overlapping in the T_2 distributions are well separated in D-T_2 correlation maps (Fig. 6, right), illustrating by example of different types of cheese that the quality of dairy products can be assessed by 1D and 2D Laplace NMR using simple hardware [66, 67]. It is worth noting that with stray-field sensors this type of food quality assessment can also be conducted on packed foods without drawing samples and without damage to the paper or plastic packaging material [58].

Biological Tissue

The success of MRI gives ample proof that biological tissues are perfect candidates for analysis by NMR relaxometry at moderate field strengths, because the contrast in human MRI is defined largely by spin density and relaxation parameters [68, 69]. Biological tissues are assemblies of cells from animals and plants. Examples are certain types of food, skin, tendon, cartilage, bone, fruit, vegetables, grains, wood, and trees. All of them contain water in different states and sugar- or protein-based macromolecules that give rise to ^{1}H NMR signals which are easily measured by compact or mobile low-field NMR instruments. Stray-field instruments are well suited for studying surface-near phenomena, in particular the skin (Fig. 7a) [30, 70–72], and bear promise for diagnosing tendon and cartilage pathologies [73], while C-shaped center-field magnets and Halbach magnets, in particular openable ones like the NMR cut-open, uniform, force free (CUFF) magnet, are employed in plant studies [74–76]. Here the mobility and lower price of compact instruments enable systematic and simultaneous studies in greenhouses and outdoors of growth cycles in dependence of environmental impact factors (Fig. 7b, c) [72, 77, 78] as well the cost-efficient assessment of harvest quality [79–81]. A tabletop instrument has

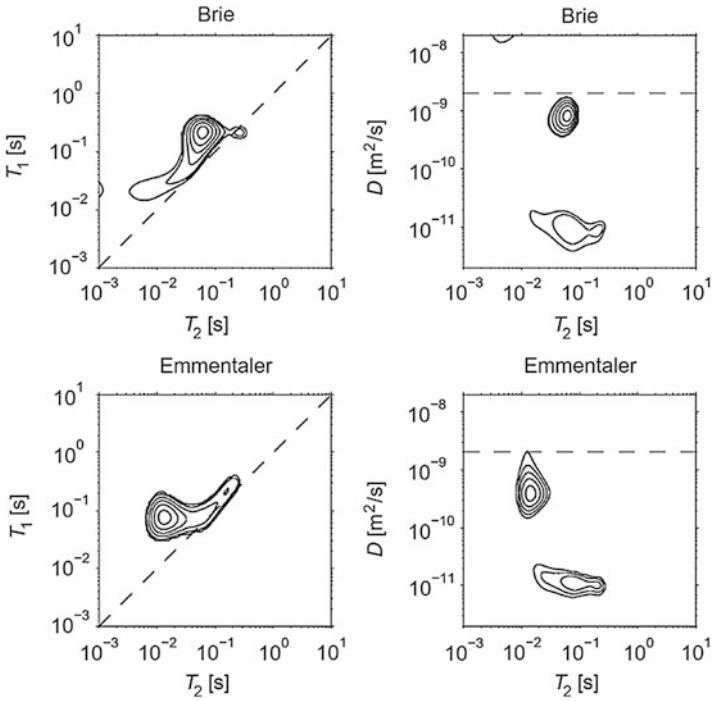

Fig. 6 2D Laplace NMR of cheese (Adapted with permission from [66]). ^{1}H T_1-T_2 (*left*) and D-T_2 (*right*) distributions of a soft cheese (*Brie*) and a hard cheese (*Emmentaler*) acquired at 5 MHz. The *dashed lines* in the T_1-T_2 distributions indicate $T_1 = T_2$, whereas in the D-T_2 distributions, they indicate the diffusion coefficient of free water

also been employed in elastographic measurements of small tissue samples to determine the storage and loss moduli [82]. A simple and valuable application of mobile NMR is the quantification of moisture content, for example, in wood, which can be achieved nondestructively with stray-field instruments [83, 84].

Polymers

Soft matters like polymers and biological tissue are well suited for characterization by low-field NMR relaxometry, because they are rich in protons, the most sensitive stable NMR nucleus, and the transverse relaxation times are sufficiently long for signal acquisition. Both center-field magnets (Fig. 8a) and mobile stray-field magnets (Fig. 8b) are used for analyzing samples and for nondestructive testing, respectively. The state of the art is reported in a number of reviews covering both technologies [85] of compact tabletop NMR with center-field magnets [40, 41, 86] and nondestructive testing with mobile stray-field magnets [13, 87] separately.

Some recent representative examples are summarized in Fig. 9. In semicrystalline polymers up to three components can be distinguished in the transverse relaxation decays. These are attributed to rigid, interfacial, and mobile components, which are

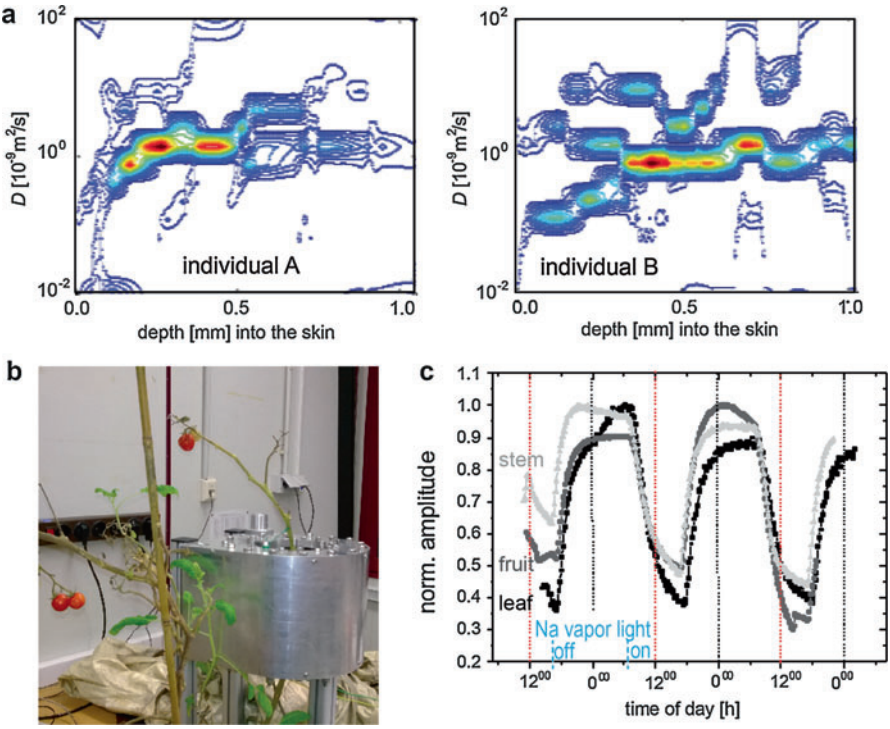

Fig. 7 Measurements of biological tissues with compact NMR instruments. (**a**) Diffusion-resolved depth profiles through the human skin of two individuals (Adapted from [30]). (**b**) Cherry tomato plant in a home-built 9.4 MHz Halbach magnet [72]. (**c**) Moisture variations in different parts of the plant as a function of light stress from a sodium vapor lamp [72]

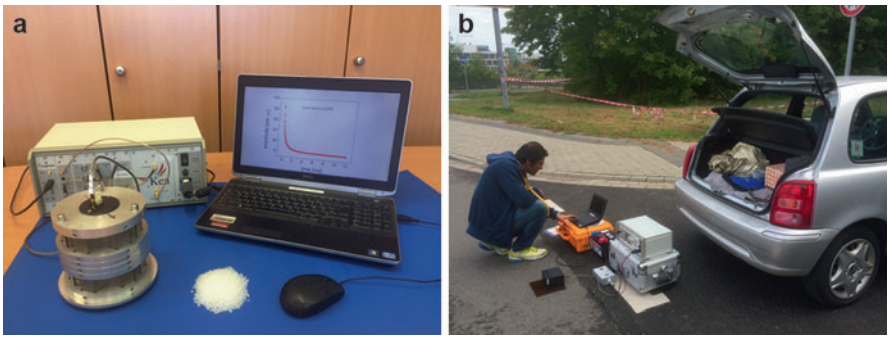

Fig. 8 NMR relaxometry of polymers and related materials. (**a**) Setup for studying morphology and aging of polymer samples with a simple permanent magnet and a compact spectrometer. (**b**) Setup for nondestructive testing of asphalt with a stray-field magnet (NMR-MOUSE) and a battery-powered, compact NMR spectrometer

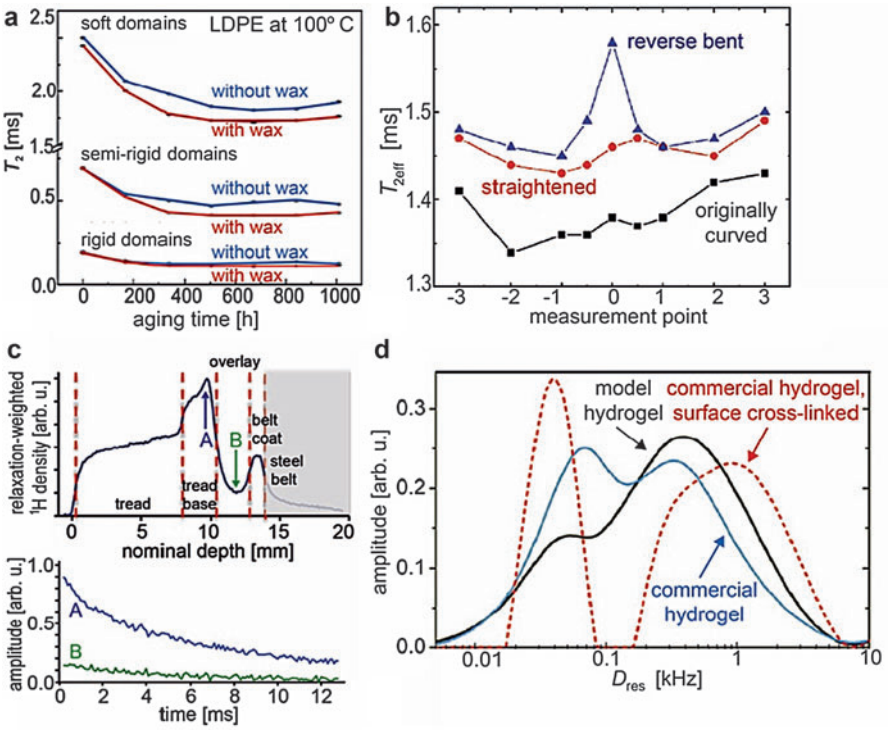

Fig. 9 NMR relaxometry of elastomer and polymer materials. (**a**) Transverse relaxation times of the different morphological components of LDPE versus time of thermo-oxidative aging at 100° C (Adapted with permission from [95]). (**b**) Transverse relaxation times along the length of an initially curved, carbon black-filled, 40 cm-long PE pipe section with a 6.3 cm outer diameter at different deformation stages (Adapted with permission from [89]). (**c**) Depth profile through an intact car tire revealing the first layers until the first steel belt (*top*). The relaxation decays at particular positions provide information about the states of curing (*bottom*). (**d**) Distributions of residual dipolar couplings for different hydrogel samples (Adapted with permission from [103])

assigned to the polymer morphology as crystalline, interfacial, and amorphous domains [85, 88]. The fractions of these domains as well as the segmental mobility within each of them change with crystallization, chemical aging, solvent ingress [89–96], the leaching of wax and additives, and deformation or pressure [97]. Summarily many of these processes can be described as aging, and each of them is associated with different time scales. The changes in segmental mobility are reported by the transverse relaxation time T_2 versus aging time for each fraction (Fig. 9a). For thermo-oxidative aging, crystallization dominates in the initial part of the aging process making the material more rigid, and chemical aging dominates at later times leading to more mobile chain segments due to chain scission [95]. In this process the presence of wax shortens the characteristic aging times. For lamellar morphologies encountered in many semicrystalline polymer materials, the domain thicknesses can

be determined by following the diffusive migration of magnetization across different domains by spin-diffusion techniques [94, 98]. Related studies concern the drying of films [99].

The importance of the amorphous domains in taking up the load upon deformation is illustrated with changes of their relaxation time along the length of a carbon black-filled 40 cm-long section of a 6.3 cm-diameter PE pipe which had been secured from a longer section rolled up on a spool. The relaxation times change noticeably when bending the weakly curved section straight and even more when bending it in reverse over a pin in the center (Fig. 9b) [89].

Due to its softness, rubber is a material very suitable for analysis by NMR relaxometry [1, 100]. For example, the NMR-MOUSE is routinely used for nondestructive inspection of tires (Fig. 9c) [101]. Depending on how the multi-echo decay signal measured at each point along the depth direction into the tire is reduced to one value, depth profiles are obtained with different contrasts that reveal the layer structure of the tire. From the relaxation decay, the cross-link density can be determined either by fitting model functions or by Laplace analysis [102]. A way to characterize the cross-link density other than by relaxation is by multi-quantum NMR [40, 41]. The existence of multi-quantum transitions rests on the residual dipole-dipole interaction D_{res}, which remains unaveraged by the anisotropic motion of the intercross-link chains in the macromolecular network. Due to the statistical nature of polymer materials, also the residual dipolar couplings are distributed [103]. For model and commercial polyelectrolyte hydrogels, the distribution of D_{res} was found by compact NMR to span two to three orders of magnitude on the frequency scale (Fig. 9d), indicating that the polymer network is composed of polymer chains ranging in mobility from highly rigid to very mobile.

Porous Media

Porous media consist of a solid matrix with pores, which, when physically connected, enable the flow of liquids and gasses through the material. Typically the pores are partially filled with a fluid that gives rise to the NMR signal, while the signal from the host matrix is not detected or suppressed due to differences in relaxation. Examples of porous media are rock, sediments, soil, cement, concrete, filters, and even biological tissues like skin, muscle, and wood. The goals in porous media studies by NMR are to determine the porosity, the pore size distribution, and the connectivity of the pore network from fluid-saturated media, the moisture content from partially saturated media, and the fluid type. Due to susceptibility differences, the applied field is inhomogeneous on the pore scale, and NMR spectra cannot be measured without sample spinning, so that the relevant information is derived from relaxation and diffusion studies including advanced 2D Laplace methods [36, 104–109]. The susceptibility-induced local field inhomogeneities scale with the field strength so that porous media are studied preferentially at low field, where mobile instruments enable measurements at the site. Whereas transverse relaxation can be measured in a single shot with multi-echo sequences, the measurement of diffusion with linear gradient fields requires indirect detection. If, however, quadratic

field profiles are employed, the distributions of displacements, i.e., the diffusion coefficient and even the surface-to-volume ratio of the host matrix, can also be determined in single-shot measurements [110, 111]. Moreover, the field inhomogeneity has so far disabled practical schemes of measuring chemical information with stray-field sensors. But chemical information is delivered with the chemical shift and the indirect coupling, and it has been demonstrated that the heteronuclear indirect coupling can be measured with double-resonance multi-echo experiments in the inhomogeneous fields of stray-field sensors [112, 113].

On-site measurements are particularly in need for well-logging applications [114–116], where 1D and 2D Laplace NMR methods have become part of the routine portfolio of measurements [117–121]. Logging tools for oil wells encompass wire line tools and logging-while-drilling tools. A wire line tool is lowered into the borehole and acquires data while being pulled up from below. For example, multi-echo trains are measured at four different depths into the borehole wall to separate wall from bulk properties of the formation (Fig. 10a) [11]. Various parameters are acquired from the formation with different instruments as a function of depth (Fig. 10b). The amplitude of the NMR echo train scales with the fluid amount in the pores and, when completely saturated, with porosity. The relaxation time distributions are obtained by Laplace inversion of the echo decay envelopes. The integral of the part of the distribution at long relaxation times provides the amount of free fluid volume that can be recovered from the formation.

The range of logging tools has been augmented in recent years to include slim-line logging tools for studying soil texture and soil moisture in the vadose zone [123–125], complementing Earth's field NMR with large surface coils for groundwater studies [126]. These on-site measurements with mobile NMR are accompanied by laboratory measurements of core plugs and soil samples [127–131] with center-field [132–134] and stray-field scanners [135] including add-ons for flooding experiments [136, 137] as well as pressure and temperature chambers to generate reservoir conditions in the laboratory [138].

Examples of other materials investigated by relaxometry are a water-saturated fuel cell membrane [139], a composite sandwich structure containing moisture [140], and filters [132]. For instance, the porosity of a diesel particulate filter (Fig. 10c) can be mapped by saturating the structure with a fluid and measuring the signal amplitude. Interesting variations of the porosity across the filter walls are revealed when scanning the porosity across the extension of the filter with the NMR-MOUSE (Fig. 10d). Moreover, the relaxation time distribution derived from multi-echo decays maps the pore size distribution obtained otherwise by cumbersome mercury intrusion porosimetry measurements (Fig. 10e).

Stray-field sensors have also proven useful in studying transient phenomena such as fluid flow [141], electrochemical reactions [142], polymerization reactions [143, 144], and the setting of white cement [145] and even of Portland cement and concrete, whereby in the latter cases the sensor was designed to be embedded in the hardening pastes [146, 147]. A related sensor is the direct insertion probe (DIP)-stick, a 2 cm-diameter logging tool that can be slid up and down a hole in a wall to monitor wall moisture over time and depth [148].

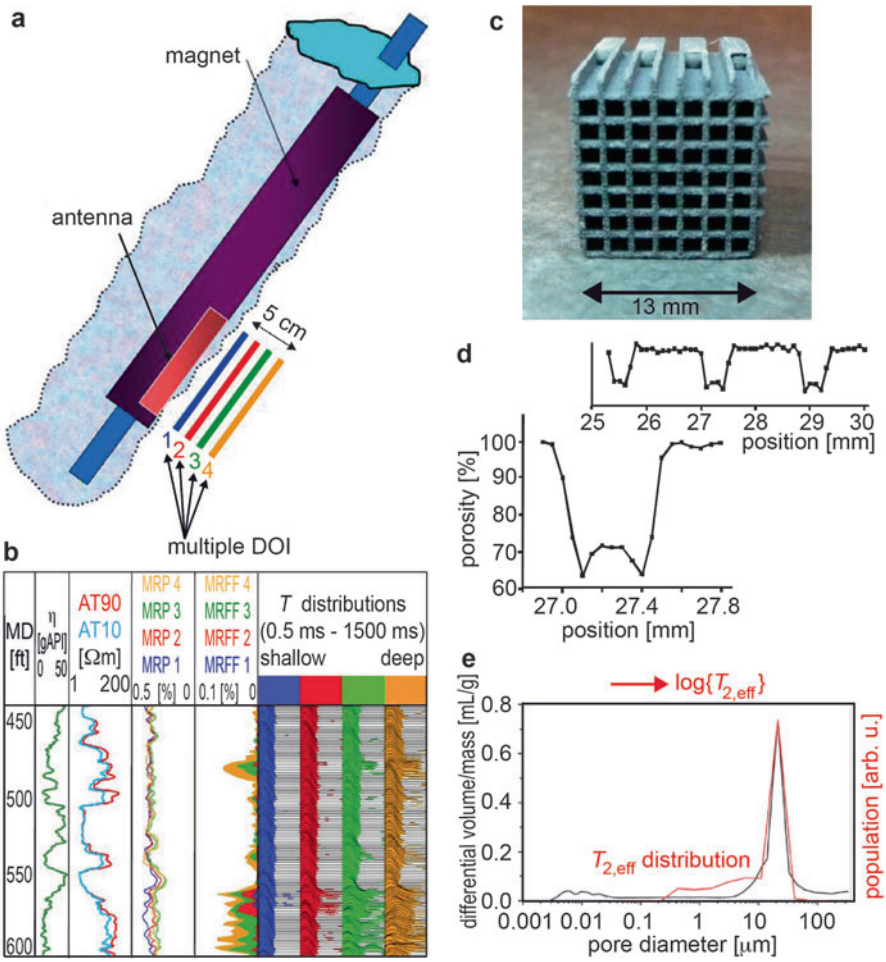

Fig. 10 Applications of mobile NMR to porous media. (**a**) Carton of a well-logging sensor with four depths of investigation (*DOI*) across a 5 cm range (Adapted with permission of Cambridge University Press from [11]). (**b**) Logging plot across an oil-bearing interval of a well from 400 to 600 ft depth showing γ-ray (track 1: viscosity) and induction logs (track 2) next to volumetric porosity (track 3), free fluid volume (track 4), and T_2 distributions (track 5) (Adapted with permission from [122]). (**c**) Section of a diesel particulate filter. (**d**) Signal amplitude across the porous ceramic array of filter cavities measured with an NMR-MOUSE. (**e**) Distribution of transverse relaxation times from water saturating pores in the ceramic walls overlaid with the pore size distribution measured with mercury intrusion porosimetry (Adapted with permission from [132])

Cultural Heritage

The study of objects of cultural heritage by compact and mobile NMR is conducted predominantly with stray-field instruments such as the NMR-MOUSE because nondestructiveness is essential in nearly all cases [1, 13, 38, 39] with the exception

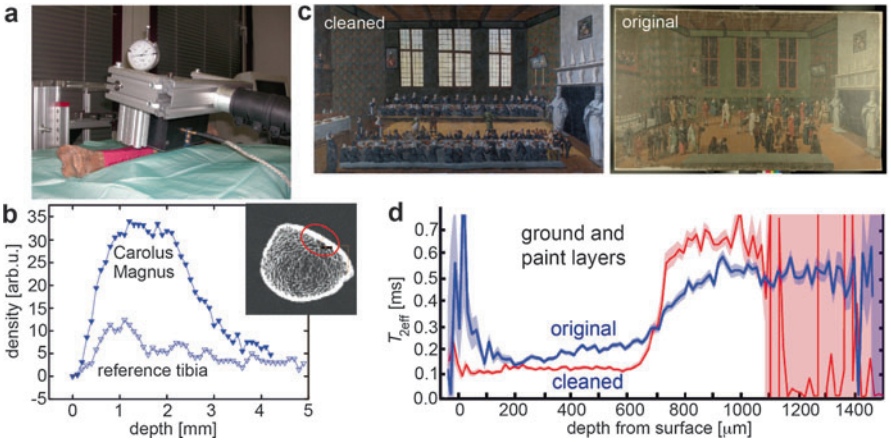

Fig. 11 Analysis of cultural heritage by mobile NMR. (**a**) Tibia of Charlemagne under investigation with the NMR-MOUSE. (**b**) Depth profiles through the tibia of Charlemagne and a reference tibia revealing a conservation treatment. The *inset* shows the position of the depth profile in a CT image [13]. (**c**) The Dinner and the Dance, Dutch, 1616. (**d**) Comparison of relaxation time depth profiles through both paintings revealing differences in the molecular mobility across the paint layers attributed to natural aging and solvent cleaning (Adapted with permission from [158])

of moisture monitoring in large building structures, a case for which the NMR DIP-stick has been designed (see above) [148]. Objectives pursued by stray-field NMR in the context of cultural heritage are moisture mapping [149, 150], contributing to the optimization of stone conservation strategies [151], studying the mortar base of wall paintings [152, 153], assessing bone degradation [13, 154], monitoring the water distribution in wooden panels such as easel paintings [155], studying the stratigraphy and binder states of paintings [156], assisting in the development of restoration techniques for easel paintings [157, 158], and studying the degradation mechanisms of parchment and leather [159–161]. The overriding goals are to understand the states of degradation, to identify the extent of past restoration and conservation measures, and to monitor the impact of conservation efforts on the state of the object. For example [1], the tibia of Charlemagne (Fig. 11a) from the treasury of the Aachen Cathedral was found to have been treated with a proton-rich conservation agent because it revealed a considerably higher proton density depth profile than that from a similarly old reference tibia (Fig. 11b), the mosaic of Neptune and Amphitrite in Herculaneum was found to have undergone an undocumented conservation treatment with wax, depth profiles through frescoes reveal the skills of the trade in making the mortar layers and also reveal similarities and differences between locations, and the artificial aging of paint by a forgerer was found to mismatch the signature of NMR relaxation times of naturally aged paint. During natural aging of paint over centuries, low molecular weight components of the binder evaporate leading to a gradient of elasticity as reported by the transverse relaxation time $T_{2\mathrm{eff}}$ across the paint layer. Solvent

cleaning of paintings may wash these components out even from deeper layers of paint, so that restored paint may have inferior mechanical properties than old original paint (Fig. 11c, d) [158].

Imaging

MRI with compact instruments largely employs permanent center-field magnets with imaging modalities similar to those of high-field MRI instruments, while mobile MRI often addresses the measurement of 1D depth profiles with stray-field magnets [1, 2, 162–164]. One-dimensional depth profiles are measured with stray-field devices by placing the sensitive slice into the object and retracting the magnet in incremental steps for each new measurement [13, 21, 22]. In this way the pixels of the depth profile are acquired in real space, whereas Fourier imaging measures the imaging information in Fourier space or $\boldsymbol{k}$-space. The contrast accessible by stray-field MRI is essentially the same as that obtainable with center-field magnets, but macroscopic anisotropy can be probed more easily with stray-field sensors because the object size is not limited by the opening of the magnet [165]. If the stray-field gradient is constant across the volume of the slice, then the Fourier transform of an echo acquired with a stray-field sensor provides a frequency-encoded 1D image [1, 30, 71].

Skin is an object readily evaluated with stray-field and related sensors, because thin layers in soft tissue can well be resolved with the high gradients of the order of 10 T/m (Fig. 8c) [30, 71, 166, 167]. Another major field of interest of mobile and compact MRI concerns plants as another type of biological tissue [168, 169]. Mobile instruments with center-field magnets have been developed to study trees (Fig. 12a) and plants in greenhouses and in their natural environments to observe transport in vessels as a function of climatic, seasonal, and temporal conditions such as light and nutrient supply [74–76, 170–173] as well as for phenotyping [174]. But also the

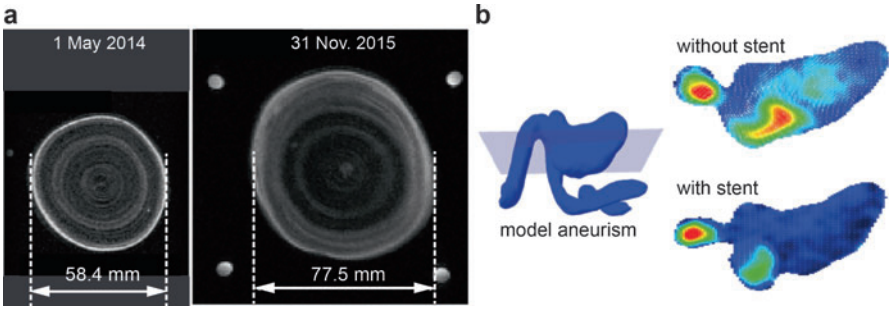

Fig. 12 Magnetic resonance imaging with compact instruments. (**a**) Spin-echo images across the trunk of a *Zelkova serrata* tree measured on 1 May 2015 and 31 Nov. 2015 (Adapted with permission from [171]). (**b**) Slice-selective velocity vector images of water flowing through an aneurism model without and with a stent. The stent suppresses the vortex motion in the aneurism sack. The color-coded velocity scale ranges from 0 to 150 mm/s (Adapted with permission from [193])

study of food ripening and disease is a matter that is being tackled with the help of compact MRI instruments [175–179].

An important class of applications of tabletop MRI relates to studies of rock cores in the context of oil and gas recovery from geological formations. The low fields of compact tomographs and dedicated rock core analyzers approximate the stray fields of mobile well-logging tools. NMR imaging is particularly valuable in visualizing the flooding of cores by displacing one fluid with another [180–186] and to quantify local fluid concentrations and matrix properties [187]. Dedicated overburden equipment has been developed to study samples under the elevated pressure and temperature conditions prevalent at the recovery depths of oil wells [138, 188]. Other geophysical MRI studies address the moisture balance in upper soil layers by depth profiling with a stray-field sensor [189] and studies of riverbed dynamics [190].

Compact MRI instruments find increasing use in the chemical engineering community [2] to investigate systems with moving components for process control such as a gasket being extruded though the magnet to image its inner and outer contours [191] and the concentration distribution in a slurry [192]. Fundamental studies concern the change of intra-aneurismal flow in model aneurisms due to incorporation of a stent (Fig. 12b) [193] or the optimization of mixing processes [194, 195]. The compelling advantage of compact instruments in these scenarios is that they can be moved to the processing equipment and operated in a common laboratory environment, even in uncommon situations such as inside a cold room [196]. To improve the sensitivity, compact permanent magnets based on high T_c superconductors are being developed [197, 198], which bear great promise for a variety of tabletop applications in engineering and animal studies.

Spectroscopy

High-resolution spectroscopy with compact permanent magnets has been a challenging niche endeavor [199, 200] until the technology was found to shim the magnets assembled from permanent magnet blocks [201] and to stabilize the temperature drift. Since about the year 2012 tabletop NMR spectrometers (Fig. 2a) are available commercially from different manufacturers differing in resolution, field strength, as well as field and shim stability [6]. Despite the low field strengths of 1–2 T, not only ^{1}H spectra but also ^{13}C spectra (Fig. 13a) and an increasing variety of 2D spectra can routinely be measured with a simple click of the mouse [202].

Considerable interest in compact tabletop NMR spectrometers comes from educational institutions where NMR spectroscopy is part of the curriculum [203]. But the high-end compact instruments are suitable for research as well. In particular, online reaction monitoring by NMR spectroscopy is facilitated by the small size of the instrument, which can readily be placed inside the fume hood next to the chemical reactor [202–206]. The sensitivity is even good enough for ultrafast measurements of 2D spectra [207, 208]. Moreover, the instruments can be sufficiently robust to be operated in a production environment, and precision and accuracy meet the demands posed in process control applications [209].

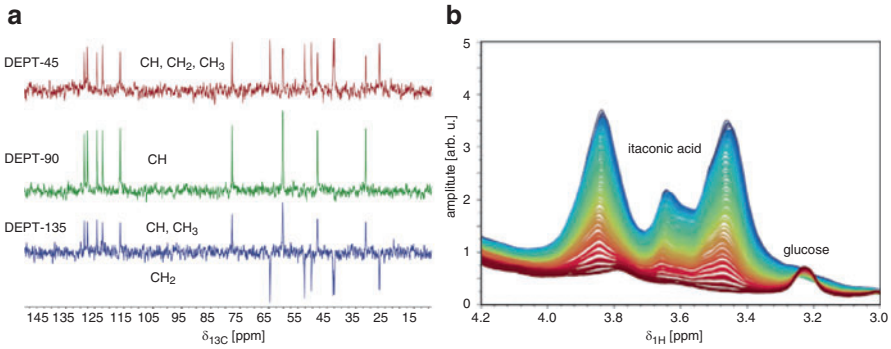

Fig. 13 NMR spectra measured at 1 T with Magritek benchtop NMR spectrometers. (**a**) ^{13}C DEPT-edited spectra of strychnine (Courtesy of Kawarpal Singh). (**b**) ^{1}H NMR spectra tracking the production of itaconic acid from sucrose by fermentation of *Ustilago maydis* observed over 60 h by continuous flow of the fermentation broth through the spectrometer (Adapted with permission from [213])

The recent availability of tabletop NMR spectrometers expands the use of NMR from studies in dedicated laboratories to general purpose laboratories and production sites. Some studies which substantiate these new opportunities are the use of ^{1}H NMR spectroscopy for monitoring the biodiesel production [210, 211], for quality control of gasoline [212], for following a hydrogenation reaction in a trickle-bed reactor [213], for fermentation processes (Fig. 13b) [214], and for polymerization processes [215]. A compact NMR spectrometer has even been employed as the primary sensor in a self-optimizing synthetic organic reactor system [216]. More challenging uses of compact NMR sensors are continuously being explored, for example, to follow electrochemical reactions [142] and to provide chemical information in size-exclusion chromatography [217, 218].

Miniaturization and Conclusions

With mobile and compact instruments being available commercially today, the quest for miniaturization continues [15–17]. So far shrinking size has gone along with shrinking price, and this trend can be expected to continue as miniaturization progresses. To be commercially viable, the applications of ultra-compact NMR devices need to address high-volume markets, which then also mean intuitive or automatic operation of the miniature instrument. The life sciences are the largest customer of NMR, be it for spectroscopy of biological macromolecules or clinical magnetic resonance imaging. The applications of miniature NMR instruments are therefore expected to also be found in the life sciences with a demand created by a large fraction of the population. This path is already being explored with body fluid analyzers based on NMR relaxometry for detection of functionalized paramagnetic compounds that bind to disease markers [219–225] with lab-on-a chip technology

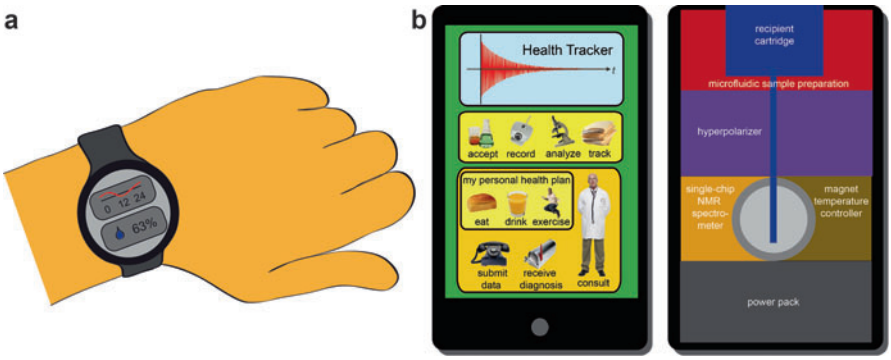

Fig. 14 NMR health trackers. (**a**) Stray-field sensor measuring skin as a reporter for diet, exercise, and disease. (**b**) Metabolomic analyzer of body fluids (Adapted with permission from [1])

[226–228], envisioning handheld NMR-based point-of-care diagnostic tools [17, 229–231].

Two further lines of applications come to mind, one being a device like a health tracker and the other a metabolomic analyzer. Health trackers are worn on the wrist or perhaps the ankle and can be imagined to contain a stray-field sensor to monitor skin as a reporter of diet, exercise, and disease (Fig. 14a) [232]. The distribution of translational diffusion coefficients appears to be one parameter particularly sensitive to the state of the skin (Fig. 8c) [30]. Yet the stray-field of the magnet poses a permanent hazard for the wearer, so that the wearers will not be ordinary people, but a particular group struck by a disease condition, which requires frequent or permanent monitoring. The other application could be a metabolomic analyzer which collects low-field spectra of body fluids [1, 233, 234] like saliva and urine but also serum and cerebrospinal fluid. Metabolomic analysis of body fluids is a rapidly growing field in high-field NMR spectroscopy [235–239] along with mass spectrometry. From 1D ^{1}H NMR spectra, it is possible to extract a disease signature by statistical analysis so that ^{1}H NMR spectroscopy could assume a key role in disease diagnosis [238, 239]. While this can be said for high-field NMR spectroscopy, the two main challenges for low-field spectroscopy at 0.5–1.5 T field strength are as follows: (1) Compared to 400 MHz ^{1}H NMR frequency, the sensitivity at 40 MHz is about a factor of 100 lower so that 10^{4} times more scans are needed to obtain spectra with the same signal-to-noise ratio. (2) The frequency dispersion of the chemical shift range is 10 times smaller, so that the signal overlap is even more than at high field.

Both challenges can be addressed by hyperpolarization [240, 241], whereby the selectivity of signal amplification can be taken advantage of for spectral simplification to address the issue of spectral crowding due to lower frequency dispersion of the chemical shift. The techniques currently most promising in this regard are the use of hyperpolarized xenon [242], dynamic nuclear polarization (DNP) [243], and parahydrogen [244]. For metabolomic studies at low field, chemical selectivity in

hyperpolarization can be achieved with xenon biosensors attached to molecules that bind to disease markers [245] and with suitable polarization catalysts that selectively transfer spin order from para-hydrogen to target molecules [244], while the selectivity of DNP spin labels is less pronounced.

A necessity for health tracking by metabolomic analysis is the widespread availability of suitable body fluid analyzers. With respect to NMR, a dense network of high-field spectrometers can be set up in local centers to track the evolution of the personal metabolomic NMR fingerprint against one's own history or the population average. But a centralized scheme requires the body fluid samples to be delivered to the center in regular time intervals. A decentralized scheme would require personal body fluid analyzers to be affordable and simple to use by everyone at home. It is the latter scenario (Fig. 14b), for which the puzzle of hardware components is on the road to completion. For example, optical hyperpolarization and NMR detection of ^{129}Xe have been realized on a microfluidic chip [246]; in pursuit of miniaturizing magnets, concepts for constructing small spectroscopy-grade magnets with homogeneous fields accounting for imperfection of magnet components have been found to be superior to concepts based on perfection of magnet components [247], and shimming by ablation on the atomic scale promises ultimate precision [248], so that residual and temperature-dependent magnetic field inhomogeneities can be reduced by novel concepts of electrical shimming [249, 250]. Despite intriguing alternatives such as optical detection [251, 252], inductive detection remains the scheme most explored in the context of miniaturization [253–255], where tuning to the low resonance frequencies of NMR with permanent magnets is enabled with sacrificial inductances [219], which, when fitted with a high-quality factor, can significantly boost the detection sensitivity [256]. Last but not least, individual components of the spectrometer as well as the entire circuitry have been miniaturized to chip-size components [257, 258] and already been demonstrated to work even for NMR spectroscopy with a compact magnet the size of a human fist [16, 259].

The conclusion is that most of the puzzle pieces are there on a proof-of-principle level to build miniature NMR spectrometers for the mass market. Yet even if the hardware becomes available, the application needs to be developed, which, for example, could be low-field ^{1}H NMR spectroscopy for metabolomic analysis.

Despite the effort of the author to address the most important developments in mobile and compact NMR, the field has grown to such enormous extent in the last years that important references may be missing in this review. Nevertheless, it is hoped that this overview provides some inspiring insights to the reader to engage in this exciting field of magnetic resonance.

References

1. Blümich B, Haber-Pohlmeier S, Zia W. Compact NMR. Berlin: de Gruyter; 2014.
2. Johns M, Fridjonson EO, Vogt S, Haber A. Mobile NMR and MRI: developments and applications. Cambridge: Royal Society of Chemistry; 2015.

3. Blümich B, Pretsch E. Compact NMR, Trends in analytical chemistry: Part A. Amsterdam: Elsevier; 2016.
4. Danieli E, Blümich B, Casanova F. Mobile nuclear magnetic resonance. In: Harris RK, Wasylishen RE, editors. eMagRes. Chichester: Wiley; 2012.
5. Danieli E, Blümich B, Casanova F. Mobile NMR. In: Simpson MJ, Simpson AJ, editors. NMR spectroscopy: a versatile tool for environmental research. New York: Wiley; 2014. p. 149–65.
6. Blümich B. Miniature and tabletop nuclear magnetic resonance spectrometers. In: Meyers RA, editor. Encyclopedia of analytical chemistry. Chichester: Wiley; 2016. doi:10.1002/9780470027318.a9458.
7. van Putte K, van den Enden J. Fully automated determination of solid fat content by pulsed NMR. J Am Oil Chem Soc. 1974;51:316–20.
8. Barker PJ, Stronks HJ. Application of the low resolution pulsed NMR "Minispec" to analytical problems in the food and agriculture industries. In: Finley JW, Schmidt SJ, Serianni AS, editors. NMR applications in biopolymers. Boston: Springer; 1990.
9. Jackson JA, Burnett LJ, Harmon F. Remote (inside-out) NMR. III. Detection of nuclear magnetic resonance in a remotely produced region of homogeneous magnetic field. J Magn Reson. 1980;41:411–21.
10. Coates GR, Xiao L, Prammer MG. NMR logging principles and applications. Houston: Halliburton Energy Service; 1999.
11. Hürlimann M, Heaton NJ. NMR well logging. In: Johns M, Fridjonsson EO, Vogt S, Haber A, editors. Mobile NMR and MRI: developments and applications. Cambridge: Royal Society of Chemistry; 2015. p. 11–85.
12. Matzkanin GA. A review of nondestructive testing of composites using NMR. In: Höller P, Dobmann G, Ruud CO, Green RE, editors. Nondestructive characterization of materials. Berlin: Springer; 1989. p. 655–69.
13. Blümich B, Perlo J, Casanova F. Mobile single-sided NMR. Prog Nucl Magn Reson Spectrosc. 2008;52:197–269.
14. Blümich B, Casanova F. Mobile NMR. In: Webb G, editor. Modern magnetic resonance. Berlin: Springer; 2008. p. 373–82.
15. Zalesskiy SS, Danieli E, Blümich B, Ananikov VP. Miniaturization of NMR systems: desktop spectrometers, microcoil spectroscopy, and "NMR on a chip" for chemistry, biochemistry, and industry. Chem Rev. 2014;114:5641–94.
16. Ha D, Sun N, Ham D. Next generation multidimensional NMR spectrometer based on semiconductor technology. eMagRes. 2015;4:117–26. doi:10.1002/9780470034590.emrstm1421.
17. Issadore D, Westervelt RM, editors. Point-of-care diagnostics on a Chip. Heidelberg: Springer; 2013.
18. Soltner H, Blümler P. Dipolar Halbach magnet stacks made from identically shaped permanent magnets for magnetic resonance. Concepts Magn Reson. 2010;36A:211–22.
19. Blümler P, Casanova F. Hardware developments: Halbach magnet arrays. In: Johns M, Fridjonsson EO, Vogt S, Haber A, editors. Mobile NMR and MRI: developments and applications. Cambridge: Royal Society of Chemistry; 2015. p. 133–57.
20. Demas V, Prado PJ. Compact magnets for magnetic resonance. Concepts Magn Reson. 2009;34A:48–59.
21. Casanova F, Perlo J, Blümich B. Single-sided NMR. Berlin: Springer; 2011.
22. Casanova F, Perlo J, Blümich B. Depth profiling by single-sided NMR. In: Stapf S, Han S-I, editors. NMR imaging in chemical engineering. Weinheim: Wiley-VCH; 2006. p. 107–22.
23. Blümler P, Casanova F. Hardware developments: single-sided magnets. In: Johns M, Fridjonsson EO, Vogt S, Haber A, editors. Mobile NMR and MRI: developments and applications. Cambridge: Royal Society of Chemistry; 2015. p. 110–32.
24. Perlo J, Casanova F, Blümich B. Advances in single-sided NMR. In: Webb G, editor. Modern magnetic resonance. Berlin: Springer; 2008. p. 1523–7.

25. Mitchell J, Blümler P, McDonald PJ. Spatially resolved nuclear magnetic resonance studies of planar samples. Prog Nucl Magn Reson Spectrosc. 2006;48:161–81.
26. Blümich B, Rehorn C, Zia W. Magnets for small-scale and portable NMR. In: Korvink J, Anders J, editors. Micro and nano scale NMR: technologies and systems. New York: Wiley; 2016. p. xxx–xxx.
27. Perlo J, Casanova F, Blümich B. Ex situ NMR in highly homogeneous fields: ^{1}H spectroscopy. Science. 2007;315:1110–2.
28. Eidmann G, Savelsberg R, Blümler P, Blümich B. The NMR MOUSE: a mobile universal surface explorer. J Magn Reson A. 1996;122:104–9.
29. Perlo J, Casanova F, Blümich B. Profiles with microscopic resolution by single-sided NMR. J Magn Reson. 2005;176:64–70.
30. Van Landeghem M, Danieli E, Perlo J, Blümich B, Casanova F. Low-gradient single-sided NMR sensor for one-shot profiling of human skin. J Magn Reson. 2012;215:74–84.
31. McDowell A, Fukushima E. Ultracompact NMR: ^{1}H spectroscopy in a subkilogram magnet. Appl Magn Reson. 2008;35:185–95.
32. Danieli E, Perlo J, Blümich B, Casanova F. Small magnets for portable NMR spectrometers. Angew Chem Int Ed. 2010;49:4133–5.
33. Halbach K. Design of permanent multipole magnets with oriented rare earth cobalt material. Nucl Instrum Methods. 1980;169:1–10.
34. Blümich B. Introduction to compact NMR: a review of methods. TrAc Trends Anal Chem. 2016. doi:10.1016/j.trac.2015.12.012.
35. Ernst RR, Bodenhausen G, Wokaun A. Principles of nuclear magnetic resonance in one and two dimensions. Oxford: Clarendon; 1987.
36. Callaghan PT. Translational dynamics and magnetic resonance. Oxford: Oxford University Press; 2011.
37. Haws EJ, Hill RR, Northrope DJ. The interpretation of proton magnetic resonance spectra. London: Heyden & Sons; 1973.
38. Blümich B, Casanova F, Perlo J, Presciutti F, Anselmi C, Doherty B. Noninvasive testing of art and cultural heritage by mobile NMR. Acc Chem Res. 2010;43:761–70.
39. Capitani D, Di Tullio V, Proietti N. Nuclear magnetic resonance to characterize and monitor cultural heritage. Prog Nucl Magn Reson Spectrosc. 2012;64:29–69.
40. Saalwächter K. Microstructure and dynamics of elastomers as studied by advanced low-resolution NMR methods. Rubber Chem Technol. 2012;85:350–86.
41. Saalwächter K. Proton multiple-quantum NMR for the study of chain dynamics and structural constraints in polymeric soft materials. Prog Nucl Magn Reson Spectrosc. 2007;51:1–35.
42. Carr HY, Purcell HM. Effects of diffusion on free precession in nuclear magnetic resonance experiments. Phys Rev. 1954;94:630–8.
43. Meiboom S, Gill D. Modified spin echo method for measuring nuclear relaxation times. Rev Sci Instrum. 1958;29:688–91.
44. Bergman E, Yeredor A, Nevo U. An estimation method for improved extraction of the decay curve signal from CPMG-like measurements with a unilateral scanner. J Magn Reson. 2014;245:87–93.
45. Borneman TW, Hürlimann MD, Cory DG. Application of optimal control to CPMG refocusing pulse design. J Magn Reson. 2010;207:220–33.
46. Marble A. Optimization of echo amplitudes resulting from a series of 90° pulses in an inhomogeneous static field. J Magn Reson. 2012;216:37–42.
47. Mandal S, Oh S, Hürlimann MD. Absolute phase effects on CPMG-type pulse sequences. J Magn Reson. 2015;261:121–32.
48. Hürlimann MD. Ex situ measurement of one- and two-dimensional distribution functions. In: Casanova F, Perlo J, Blümich B, editors. Single-sided NMR. Berlin: Springer; 2011. p. 57–86.

49. Voda MA, Van Duynhoven J. Bench-top NMR – food: solid fat content determination and emulsion droplet sizing. In: Johns M, Fridjonson EO, Vogt S, Haber A, editors. Mobile NMR and MRI: developments and applications. Cambridge: Royal Society of Chemistry; 2015. p. 86–109.
50. Cudaj M, Hofe T, Wilhelm M, Vargas MA, Guthausen G. Medium resolution NMR at 20 MHz: possibilities and challenges. In: Renou J-P, Belton P, Webb GA, editors. Magnetic resonance in food science. An exciting future. Cambridge: Royal Society of Chemistry; 2011. p. 46–56.
51. Bernewitz R, Horvat M, Schuchmann H-P, Guthausen G. Structures in food: possibilities of imaging and diffusometry. In: van Duynhoven J, Belton P, Webb GA, editors. Magnetic resonance in food science. Food for thought. Cambridge: Royal Society of Chemistry; 2013. p. 91–102.
52. Guthausen G. Analysis of food and emulsions. TrAC Trends Anal Chem. 2016. doi:10.1016/j.trac.2016.02.011.
53. van Duynhoven J, Voda A, Witek M, Van As H. Time-domain NMR applied to food products. Annu Rep NMR Spectrosc. 2010;69:145–97.
54. Trezza E, Haiduc AM, Goudappel GJW, van Duynhoven JPM. Rapid phase compositional assessment of lipid-based food products by time domain NMR. Magn Reson Chem. 2006;44:1023–30.
55. Todt H, Burk W, Guthausen G, Guthausen A, Kamlowski A, Schmalbein D. Quality control with time-domain NMR. Eur J Lipid Sci Technol. 2001;103:835–40.
56. Kim SM, McCarthy MJ. Investigation of olive accession using nuclear magnetic resonance. J Agric Life Sci. 2010;41:75–82.
57. Bernewitz R, Guan X, Guthausen G, Wolf F, Schuchmann H-P. PFG-NMR on double emulsions: a detailed look into molecular processes. In: Renou J-P, Belton P, Webb GA, editors. Magnetic resonance in food science. An exciting future. Cambridge: Royal Society of Chemistry; 2011. p. 46–56.
58. Guthausen G, Todt H, Burk W, Schmalbein D, Kamlowski A. Time-domain NMR in quality control: (C) single-sided NMR in foods. In: Webb GA, editor. Modern magnetic resonance. Berlin: Springer; 2006. p. 1873–97.
59. Petrov OV, Hay J, Balcom BJ. Fat and moisture content determination with unilateral NMR. Food Res Int. 2008;7:758–64.
60. Veliyullin E, Masthikin IV, Marble AE, Balcom BJ. Rapid determination of fat content in packed products by unilateral NMR. J Sci Food Agric. 2008;88:2563–7.
61. Nakashima Y. Development of a single-sided nuclear magnetic resonance scanner for the in vivo quantification of live cattle marbling. Appl Magn Reson. 2015;46:593–606.
62. Provencher SW. A constrained regularization method for inverting data represented by linear algebraic or integral equations. Comput Phys Commun. 1982;27:213–27.
63. Borgia GC, Brown RJS, Fantazzini P. Uniform-penalty inversion of multiexponential decay data. J Magn Reson. 2000;147:273–85.
64. Lamanna R. On the inversion of multicomponent NMR relaxation and diffusion decays in heterogeneous systems. Concepts Magn Reson. 2005;26A:87–90.
65. Venkataramanan L, Song YQ, Hürlimann MD. Solving Fredholm integrals of the first kind with tensor product structure in 2 and 2.5 dimensions. IEEE Trans Signal Process. 2002;50:1017–26.
66. Song Y-Q. A 2D NMR method to characterize granular structure of dairy products. Prog Nucl Magn Reson Spectrosc. 2009;55:324–34.
67. Hürlimann MD, Burcaw L, Song Y-Q. Quantitative characterization of food products by two-dimensional D-T_2 and T_1-T_2 distribution functions in a static gradient. J Colloid Interface Sci. 2006;297:303–11.
68. Callaghan PT. Principles of nuclear magnetic resonance microscopy. New York: Oxford University Press; 1991.
69. Blümich B. NMR imaging of materials. Oxford: Clarendon; 2000.

70. Blümich B. Applications in biology and medicine. In: Casanova F, Perlo J, Blümich B, editors. Single-sided NMR. Berlin: Springer; 2011. p. 187–202.
71. Danieli E, Blümich B. Single-sided magnetic resonance depth profiling in biological and materials science. J Magn Reson. 2013;299:142–54.
72. Oligschläger D. Advances in compact stray-field NMR. Aachen: Dissertation RWTH Aachen University; 2015.
73. Rössler E, Mattea C, Stapf S. Feasibility of high-resolution one-dimensional relaxation imaging at low field using a single-sided NMR scanner applied to articular cartilage. J Magn Reson. 2015;251:43–51.
74. Windt CW, Blümler P. A portable NMR sensor to measure dynamic changes in the amount of water in living stems or fruit and its potential to measure sap flow. Tree Physiol. 2015;35:366–75.
75. Windt CW, Soltner H, van Dusschoten D, Blümler P. A portable Halbach magnet that can be opened and closed without force: the NMR-CUFF. J Magn Reson. 2011;208:27–33.
76. Jones M, Aptaker PS, Cox J, Gardiner BA, McDonald PJ. A transportable magnetic resonance imaging system for *in-situ* measurements of living trees: the tree hugger. J Magn Reson. 2012;218:133–40.
77. Geya Y, Kimura T, Fujisaki H, Terada Y, Kose K, Haishi T, et al. Longitudinal NMR parameter measurements of Japanese pear fruit during the growing process using a mobile magnetic resonance imaging system. J Magn Reson. 2013;226:45–51.
78. Zhang L, McCarthy MJ. NMR relaxometry study of development of freeze damage in mandarin orange. J Sci Food Agric. 2015;96:3133–9.
79. Le P, Zhang L, Lim V, McCarthy MJ, Nitin N. A novel approach for measuring resistance of *Escherichia coli* and *Listeria monocytogenes* to hydrogen peroxide using label-free magnetic resonance imaging and relaxometry. Food Control. 2015;50:560–7.
80. Zhang L, McCarthy MJ. Assessment of pomegranate postharvest quality using nuclear magnetic resonance. Postharvest Biol Technol. 2013;77:59–66.
81. Kirtil E, Oztop HM, Sirjariyawat A, Ngamchuachit P, Barrett DM, McCarthy MJ. Effect of pectin methyl esterase (PME) and $CaCl_2$ infusion on the cell integrity of fresh-cut and frozen-thawed mangoes: an NMR relaxometry study. Food Res Int. 2014;66:409–16.
82. Ipek-Ugay S, Direßle T, Ledwig M, Guo J, Hirsch S, Sack I, et al. Tabletop magnetic resonance elastography for the measurement of viscoelastic parameters of small tissue samples. J Magn Reson. 2015;251:13–8.
83. Macmillan B, Veliyulin E, Lamason C, Balcom BJ. Quantitative magnetic resonance measurements of low moisture content wood. Can J For Res. 2011;41:2158–62.
84. Lamason C, Macmillan B, Balcom B, Leblonz B. Water content measurement in black spruce and aspen sapwood with benchtop and portable magnetic resonance devices. Wood Mat Eng. 2015;10:86–93.
85. Adams A. Analysis of solid technical polymers by compact NMR. TrAC Trends Anal Chem. 2016. doi:10.1016/j.trac.2016.04.003.
86. Schäler K, Roos M, Micke P, Golitsyn Y, Seidlitz A, Thurn-Albrecht T, et al. Basic principles of static proton low-resolution spin diffusion NMR in nanophase-separated materials with mobility contrast. Solid State Nucl Magn Reson. 2015;72:50–63.
87. Kolz J. Applications in materials science and cultural heritage. In: Casanova F, Perlo J, Blümich B, editors. Single-sided NMR. Berlin: Springer; 2011. p. 203–22.
88. Maus A, Hertlein C, Saalwächter K. A robust proton NMR method to investigate hard/soft ratios, crystallinity, and component mobility in polymers. Macromol Chem Phys. 2006;207:1150–8.
89. Adams A, Adams M, Blümich B, Kocks H-J, Hilgert O, Zimmermann S. Nondestructive testing procedure for evaluation of fracture-mechanically relevant abnormalities in partially crystalline polymers. 3R Int. 2010;4:216–25.

90. Adams A, Piechatzek A, Schmitt G, Siegmund G. Single-sided nuclear magnetic resonance for condition monitoring of cross-linked polyethylene exposed to aggressive media. Anal Chim Acta. 2015;887:163–71.
91. Blümich B, Adams-Buda A, Baias M. Alterung von Polyethylen: Zerstörungsfreies Prüfen mit mobiler magnetischer Resonanz. GWF Gas Erdgas. 2007;148:95–8.
92. Kwamen R, Blümich B, Buda A. Estimation of self-diffusion coefficients of small penentrants in semicrystaline polymers using single-sided NMR. Macromol Rapid Commun. 2012;33:943–7.
93. Reuvers NJW, Huinink HP, Fischer HR, Adan OG. Quantitative water uptake study in thin nylon-6 films with NMR imaging. Macromol. 2012;45:1937–45.
94. Hedesiu C, Demco DE, Kleppinger R, Adams-Buda A, Blümich B, Remerie K, Litvinov VM. The effect of temperature and annealing on the phase composition, molecular mobility and the thickness of domains in high-density polyethylene. Polymer. 2007;48:763–77.
95. Teymouri Y, Kwamen R, Blümich B. Aging and degradation of LDPE by compact NMR. Macromol Mat Chem. 2015;300:1063–2070.
96. Teymouri Y, Adams A, Blümich B. Compact low-field NMR: unmasking morphological changes from solvent-induced crystallization in polyethylene. Eur Polym J. 2016;80:48–57.
97. Sun N, Wenzel M, Adams A. Morphology of high-density polyethylene pipes stored under hydrostatic pressure at elevated temperature. Polymer. 2014;55:3792–800.
98. Campise F, Roth LE, Acosta RH, Villar MA, Vallés EM, Monti GA, et al. Contribution of linear guest and structural pendant chains to relaxation dynamics in model polymer networks probed by time-domain ^{1}H NMR. Macromol. 2016;49:387–94.
99. Doughty PJ, McDonald PJ. Drying coatings and other applications with GARField. In: Stapf S, Han S-I, editors. NMR imaging in chemical engineering. Weinheim: Wiley-VCH; 2006. p. 89–106.
100. Zheng X, Xianjun C, Kaikai M, Yunfeng X. Novel unilateral NMR sensor for assessing the aging status of silicone rubber insulator. IEEE Sens J. 2016;16:1168–75.
101. Blümich B. Compact NMR helps tire, rubber testing. Rubber Plastic News, 8 Sept 2014. p. 31–3.
102. Chalcea RI, Fechete R, Culea E, Demco DE, Blümich B. Distributions of transverse relaxation times for soft solids measured in strongly inhomogeneous magnetic fields. J Magn Reson. 2009;196:179–90.
103. Höpfner J, Guthausen G, Saalwächter K, Wilhelm M. Network structure and inhomogeneities of model and commercial polyelectrolyte hydrogels as investigated by low-field proton NMR techniques. Macromolecules. 2014;47:4251–65.
104. Song YQ. Magnetic resonance in porous media (MRPM): a perspective. J Magn Reson. 2013;229:12–24.
105. Hürlimann MD, Song Y-Q, Fantazzini P, Bortolotti V. Magnetic resonance in porous media. AIP conference proceedings 1081. New York: Am Inst Phys; 2008.
106. Xie R, Xiao L. Advanced fluid typing methods for NMR logging. Pet Sci. 2011;8:163–9.
107. Paciok E, Haber A, van Landeghem M, Blümich B. Relaxation exchange in nanoporous silica by low-field NMR. Z Physiol Chem. 2012;226:1243–57.
108. Fleury M, Soualem J. Quantitative analysis of diffusional pore coupling from T_2-store-T_2 NMR experiments. J Colloid Interface Sci. 2009;336:250–9.
109. Van Landeghem M, Haber A, d'Espinose de Lacaillerie J-B, Blümich B. Analysis of multisite 2D relaxation exchange NMR. Concepts Magn Reson. 2010;36A:153–69.
110. Kittler WC, Galvosas P, Hunter MW. Parallel acquisition of q-space using second order magnetic fields for single-shot diffusion measurements. J Magn Reson. 2014;244:46–52.
111. Kittler WC, Obruchkov S, Galvosas P, Hunter MW. Pulsed second order field NMR for real time PGSE and single-shot surface to volume ratio measurements. J Magn Reson. 2014;247:42–9.
112. Mandal S, Song Y-Q. Heternuclear J-coupling measurements in grossly inhomogeneous magnetic fields. J Magn Reson. 2015;255:15–27.

113. Donaldson M, Freed D, Mandal S, Song Y-Q. Chemical analysis using low-field magnetic resonance. TrAC Trends Anal Chem. 2016. doi:10.1016/j.trac.2016.03.008.
114. Hirasaki GJ. NMR applications in petroleum reservoir studies. In: Stapf S, Han S-I, editors. NMR imaging in chemical engineering. Weinheim: Wiley-VCH; 2006. p. 321–39.
115. Hu H-T, Xiao L. Investigation characteristics of NMR wireline logging tools. Chin J Magn Reson. 2010;27:572. ISSN 1000–4556.
116. Xiao L, Liu K. Characteristics of the nuclear magnetic resonance logging response in fracture oil and gas reservoirs. New J Phys. 2011;13:045003.
117. Liu H, Xiao L, Guo B, Zhang Z, Zong F, Deng F, et al. Heavy oil component characterization with multi-dimensional unilateral NMR. Pet Sci. 2013;10:402–7.
118. Neudert O, Stapf S, Mattea C. Diffusion exchange NMR spectroscopy in inhomogeneous magnetic fields. J Magn Reson. 2011;208:256–61.
119. Song Y-Q. Novel two dimensional NMR of diffusion and relaxation for material characterization. In: Stapf S, Han S-I, editors. NMR imaging in chemical engineering. Weinheim: Wiley-VCH; 2006. p. 163–82.
120. Xiao L, Liu H, Deng F, Zhang Z, An T, Zong F, Anferov V, Anferova S. Probing internal gradients dependence in sandstones with multi-dimensional NMR. Microporous Mesoporous Mater. 2013;178:90–3.
121. Xiao L, Liao G, Xie R, Wang Z. Inversion of NMR relaxation measurements in well logging. In: Codd SL, Seymour D, editors. Magnetic resonance microscopy. Weinheim: Wiley-VCH; 2009. p. 501–17.
122. Heaton NJ, Freedman R, Karminik R, Taherian R, Walter K, DePavia L. Applications of a new-generation NMR wireline logging tool. In: SPE7740, editor. Presented at the 77th SPE Annual Technical Conference and Exhibition, San Antonio. 2002.
123. Perlo J, Danieli E, Perlo J, Blümich B, Casanova F. Optimized slim-line logging tool to measure soil moisture in situ. J Magn Reson. 2013;233:74–9.
124. Sucre O, Pohlmeier A, Minière A, Blümich B. Low-field NMR logging sensor for measuring hydraulic parameters of model soils. J Hydrol. 2011;406:30–8.
125. Walsh D, Turner P, Grunewald E, Zhang H, Butler Jr JJ, Reboulet E, et al. A small-diameter NMR logging tool for groundwater investigations. Ground Water. 2013;51:914–26.
126. Hertrich M. Imaging of groundwater with nuclear magnetic resonance. Progr Nucl Magn Reson Spectrosc. 2008;53:227–48.
127. Van As H, Homan N, Vergeldt FJ, Windt CW. MRI of water transport in the soil-plant-atmosphere continuum. In: Codd SL, Seymour D, editors. Magnetic resonance microscopy. Weinheim: Wiley-VCH; 2009. p. 315–30.
128. Conte P, Berns AE, Pohlmeier A, Alonzo G, editors. Special issue: Applications and new developments of magnetic resonance techniques in soil science. Open Magn Reson J. 2010;3. ISSN 1874–7898.
129. Jaeger F, Shchegolikhina A, Van As H, Schaumann GE. Proton NMR relaxometry as a useful tool to evaluate swelling processes in peat soils. Open Magn Reson J. 2010;3:27–45.
130. Jaeger F, Bowe S, Van As H, Schaumann GE. Evaluation of ^{1}H NMR relaxometry for the assessment of pore-size distribution in soil samples. Eur J Soil Sci. 2009;60:1052–64.
131. Stinagciu L, Pohlmeier A, Blümler P, Weihermüller L, van Dusschoten V, Stapf S, et al. Characterization of unsaturated porous media by high-field and low-field NMR relaxometry. Water Resource Res. 2009;45:W08412.
132. Blümich B, Casanova F, Dabrowski M, Danieli E, Evertz L, Haber A, et al. Small-scale instrumentation for nuclear magnetic resonance of porous media. New J Phys. 2011;13:015003.
133. Blümich B, Mauler J, Haber A, Perlo J, Danieli E, Casanova F. Mobile NMR for geophysical analysis and materials testing. Pet Sci. 2009;6:1–7.
134. Freeman R, Anand V, Grand B, Ganesan K, Tabrizi P, Torres R, et al. A compact high-performance low-field NMR apparatus for measurement on fluids at very high pressures and temperatures. Rev Sci Instrum. 2014;85:025102–1–10.

135. García-Naranjo JC, Mastikhin IV, Colpitts BG, Balcom BJ. A unilateral magnet with an extended constant magnetic field gradient. J Magn Reson. 2010;207:337–44.
136. Qi Y, Liu N, Wang W. The observation of residual oil evolution during water flooding using NMR D-T_2 maps. Appl Magn Reson. 2015;46:1089–98.
137. Liu Z-Y, Li Y-Q, Cui M-H, Wang F-Y, Prasiddhianti AG. Pore-scale investigation of residual oil displacement in surfactant–polymer flooding using nuclear magnetic resonance experiments. Pet Sci. 2016;13:91–9.
138. Ouelette M, Li M, Liao G, Hussein EMA, Romero-Zeron L, Balcom BJ. Rock core analysis: metal core holders for magnetic resonance imaging under reservoid conditions. In: Johns M, Fridjonsson EO, Vogt S, Haber A, editors. Mobile NMR and MRI. Cambridge: Royal Society of Chemistry; 2016. p. 190–309.
139. Fechete R, Demco DE, Zhu X, Tillmann W, Möller M. Water states and dynamics in perfluorinated ionomer membranes by ^{1}H one- and two-dimensional NMR spectroscopy, relaxometry, and diffusometry. Chem Phys Lett. 2014;597:6–15.
140. Marble AE, LaPlante G, Mastikhin IV, Balcom BJ. Magnetic resonance detection of water in composite sandwich structures. NDT E Int. 2009;42:404–9.
141. Deng F, Xiao L, Liao G, Zong F, Chen W. A new approach of two-dimensional NMR relaxation measurement in flowing fluid. Appl Magn Reson. 2014;45:179–92.
142. Gomez BF, Nunes LMS, Lobo CMS, Carvalho AS, Cabeca LF, Colnago LA. In situ analysis of copper electro-deposition reaction using unilateral NMR sensor. J Magn Reson. 2015;261:83–6.
143. Hailu K, Guthausen G, Becker W, König A, Bendfeld A, Geissler E. In-situ characterization of the cure reaction of HTPB and IPDI by simultaneous NMR and IR measurements. Polym Test. 2010;29:513–9.
144. Marchi Netto A, Steinhaus J, Hausnerova B, Moeginger B, Blümich B. Time-resolved study of the photo-curing process of dental resins with the NMR-MOUSE. Appl Magn Reson. 2013;44:1027–39.
145. Van Landeghem M, d'Espinose de Lacaillerie J-B, Blümich B, Korb J-P, Bresson B. The roles of hydration and evaporation during the drying of a cement paste by localized NMR. Cem Concr Res. 2013;48:86–96.
146. Cano-Barrita PFJ, Marble AE, Balcom BJ, Garcia JC, Masthikin IV, Thomas MDA, et al. Embedded NMR sensors to monitor water loss causes by hydration in Portland cement mortar. Cem Concr Res. 2009;30:324–8.
147. Díaz-Díaz F, Cano-Barrita PFJ, Balcom BJ, Solís-Nájera SE, Rodríguez AO. Embedded NMR sensor to monitor compressive strength development and pore size distribution in hydrating concrete. Sensors. 2013;13:15985–99.
148. Oligschläger D, Kupferschläger K, Poschadel T, Watzlaw J, Blümich B. Miniature mobile NMR sensors for material testing and moisture-monitoring. Diffus Fundam. 2014;22:1–25.
149. Proietti N, Capitani D, Lamanna R, Presciutti F, Rossi E, Segre AL. Fresco paintings studied by unilateral NMR. J Magn Reson. 2005;177:111–7.
150. Di Tullio V, Proietti N, Gobbino M, Capitani D, Olmi R, Priori S, et al. Non-destructive mapping of dampness and salts in degraded wall paintings in hypogeous buildings: the case of St. Clement at mass fresco in St. Clement Basilica, Rome. Anal Bioanal Chem. 2010;396:1885–96.
151. Di Tullio V, Proietti N, Capitani D, Nicolini I, Mecchi AM. NMR depth profiling as a non-invasive analytical tool to probe the penetration depth of hydrophobic treatments and inhomogeneities in treated porous stones. Anal Bioanal Chem. 2011;400:3151–64.
152. Haber A, Blümich B, Souvorova D, Del Federico E. Ancient Roman wall paintings mapped nondestructively by portable NMR. Anal Bioanal Chem. 2011;401:1441–52.
153. Fukunaga K, Meldrum T, Zia W, Ohno M, Fuchida T, Blümich B. Nondestructive investigation of the internal structure of fresco paintings. IEEE Digit Herit. 2013;1:81–8.

154. Rühli F, Böni T, Perlo J, Casanova F, Baias M, Egarter E, et al. Non-invasive spatial tissue discrimination in ancient mummies and bones in situ by portable nuclear magnetic resonance. J Cult Herit. 2007;8:257–63.
155. Senni L, Casieri C, Bovino A, Gaetani MC, De Luca F. A portable NMR sensor for moisture monitoring of wooden works of art, particularly paintings on wood. Wood Sci Technol. 2011;43:167–80.
156. Presciutti F, Perlo J, Casanova F, Glöggler S, Miliani C, Blümich B, et al. Noninvasive nuclear magnetic resonance profiling of painting layers. Appl Phys Lett. 2008;93:033505-1–3.
157. Del Federico E, Centeno SA, Kehlet C, Currier P, Stockman D, Jerschow A. Unilateral NMR applied to the conservation of works of art. Anal Bioanal Chem. 2010;396:213–20.
158. Fife GR, Stabik B, Kelley AE, King JN, Blümich B, Hoppenbrouwers R, et al. Characterization of aging and solvent treatments of painted surfaces using single-sided NMR. Magn Reson Chem. 2015;53:58–63.
159. Masic A, Chierotti MR, Gobetto R, Martra G, Rabin I, Coluccia S. Solid-state and unilateral NMR study of deterioration of a Dead Sea Scroll fragment. Anal Bioanal Chem. 2012;402:1551–7.
160. Zhu L, Del Federico E, Llott AJ, Klokkernes T, Kehlet C, Jerschow A. MRI and unilateral NMR study of reindeer skin tanning processes. Anal Chem. 2015;87:3820–5.
161. Badea E, Sendrea C, Carsote C, Adams A, Blümich B. Unilateral NMR and thermal microscopy studies of vegetable tanned leather exposed to dehydrothermal treatment and light irradiation. Microchem J. 2016;129:158–65.
162. Stapf S, Han S-I, editors. NMR imaging in chemical engineering. Weinheim: Wiley-VCH; 2006.
163. Kose K, Haishi T, Handa S. Applications of permanent-magnet compact MRI systems. In: Codd SL, Seymour D, editors. Magnetic resonance microscopy. Weinheim: Wiley-VCH; 2009. p. 365–82.
164. Kose K. Compact MRI for chemical engineering. In: Stapf S, Han S-I, editors. NMR imaging in chemical engineering. Weinheim: Wiley-VCH; 2006. p. 77–88.
165. Rössler E, Mattea C, Mollava A, Stapf S. Low-field one-dimensional and direction dependent relaxation imaging of bovine articular cartilage. J Magn Reson. 2011;213:112–8.
166. McDonald PJ, Akhmerov A, Backhouse LJ, Pitts S. Magnetic resonance profiling of human skin in vivo using GARField magnets. J Pharm Sci. 2005;94:1850–60.
167. Ciampi E, van Ginkel M, McDonald PJ, Pitts S, Bonnist EY, Singleton S, et al. Dynamic in vivo mapping of model moisturiser ingress into human skin by GARField MRI. NMR Biomed. 2010;24:135–44.
168. Van As H, van Duynhoven J. MRI of plants and foods. J Magn Reson. 2013;229:25–34.
169. Tomiha S, Iita N, Okada F, Handa S, Kose K. Relaxation time measurements of bone marrow protons in the calcaneus using a compact MRI system at 0.2 Tesla field strength. Magn Reson Chem. 2008;60:485–8.
170. Kimura T, Geya Y, Terada Y, Kose K, Haishi T, Gemma H, et al. Development of a mobile magnetic resonance imaging system for outdoor tree measurements. Rev Sci Instrum. 2011;82:053704.
171. Nagata A, Kose K, Terada Y. Development of an outdoor MRI system for measuring flow in a living tree. J Magn Reson. 2016;265:129–38.
172. Van As H, Schenen T, Vergeldt FJ. MRI of intact plants. Photosynth Res. 2009;102:213–22.
173. Windt CW, Vergeldt FJ, de Jager PA, van As H. MRI of long-distance water-transport: a comparison of the phloem and xylem flow characteristics and dynamics in poplar, castor bean, tomato and tobacco. Plant Cell Environ. 2006;29:1715–29.
174. Rascher U, Blossfeld S, Fiorani F, Jahnke S, Jansen M, Kuhn AJ, et al. Non-invasive approaches for phenotyping of enhanced performance traits in bean. Funct Plant Biol. 2011;38:968–83.
175. van Duynhoven JPM, Goudappel GJW, Weglarz WP, Windt CW, Cabrer PR, Mohoric A, et al. Noninvasive assessment of moisture migration in food products by MRI. In: Codd SL,

Seymour D, editors. Magnetic resonance microscopy. Weinheim: Wiley-VCH; 2009. p. 331–52.
176. McCarthy MJ, Gambhir PN, Goloshevsky AG. NMR for food quality control. In: Stapf S, Han S-I, editors. NMR imaging in chemical engineering. Weinheim: Wiley-VCH; 2006. p. 471–89.
177. Milczarek RR, McCarthy MJ. Low-field MR sensors for fruit inspection. In: Codd SL, Seymour D, editors. Magnetic resonance microscopy. Weinheim: Wiley-VCH; 2009. p. 289–302.
178. Zhang L, McCarthy MJ. Black heart characterization and detection in pomegranate using NMR relaxometry and MR imaging. Postharvest Biol Technol. 2012;67:96–101.
179. Tao F, Zhang L, McCarty MJ, Beckles DM, Saltveit M. Magnetic resonance imaging provides spatial resolution of chilling injury in Micro-Tom tomato (*solanum lycopersicum* L.) fruit. Postharvest Biol Technol. 2014;97:62–7.
180. Mitchell J, Staniland J, Wilson A, Howe A, Clarke A, Fordham EJ, et al. Magnetic resonance imaging of chemical EOR in core to complement field pilot studies. Aberdeen: International Symposium, Society of Core Analysts. 2012. SCA2012–30.
181. Romero-Zeron LB, Ongsurakul S, Li L, Balcom B. Visualization of the effect of porous media wettability on polymer flooding performance through unconsolidated porous media using magnetic resonance imaging. J Pet Sci Technol. 2010;28:52–67.
182. Petrov OV, Ersland G, Balcom BJ. T_2 distribution mapping profiles with phase-encode MRI. J Magn Reson. 2011;209:39–46.
183. Mitchell J, Edwards JE, Fordham E, Stanlland J, Chassagne R, Cherukupalli PK, et al. Quantitative remaining oil interpretation using magnetic resonance: from the laboratory to the pilot. SPE EOR Conference. www.onepetro.org 2012. SPE-154704-MS. doi:10.2118/154704-MS.
184. Ferno MA, Haugen A, Graue A. Visualizing oil displacement in fractured carbonate rocks-impacts on oil recovery at different hydrostatic stress and wettability conditions. 5th US-Canada Rock Mechanics Symposium. www.onepetro.org 2010. ARMA-10-288.
185. Kwak HT, Funk JJ, Yousef AA, Balcom BJ. New insights into microscopic fluid/rock Interaction: MR-CT microscopy approach. SPE Ann Tech Conf Exhib. www.onepetro.org 2012. SPE-159194-MS. doi:10.2118/159194-MS.
186. Meybodi HE, Kharrat R, Araghi MN. Experimental studying of pore morphology and wettability effects on microscopic and macroscopic displacement efficiency of polymer flooding. J Pet Sci Technol. 2010;78:347–63.
187. Bortolotti V, Macini P, Mesini EN, Fantazzini P, Gombia M, Srisuriyachai F. Probing wettability reversal in carbonatic rocks by spatially resolved and non-resolved ^{1}H-NMR relaxation analysis. SPE Ann Tech Conf Exhib. www.onepetro.org 2010. SPE-133937-MS. doi:10.2118/133937-MS.
188. Han H, Ouellette M, MacMillan B, Goora F, MacGregor R, Green D, et al. High pressure magnetic resonance imaging with metallic vessels. J Magn Reson. 2011;213:90–7.
189. Merz S, Pohlmeier A, Vanderborght J, van Dusschoten D, Vereecken H. Moisture profiles of the upper soil layer during evaporation monitored by NMR. Water Resour Res. 2014;50:5184–95.
190. Haynes H, Lakshmanan S, Ockelford A-M, Vignaga E, Holmes WM. The emerging use of magnetic resonance imaging to study river bed dynamics. Spetrosc Eur. 2015;21:6–8.
191. Danieli E, Berdel K, Perlo J, Michaeli W, Masberg U, Blümich B, et al. Determining object boundaries from MR images with sub-pixel resolution: towards in-line inspection with a mobile tomograph. J Magn Reson. 2010;207:53–8.
192. Lavenson DM, Tozzi EJ, McCarthy MJ, Powell RL. Effective diffusivities of BSA in cellulosic fiber beds measured with magnetic resonance imaging. Cellulose. 2012;19:1085–95.
193. Perlo J, Siletta E, Danieli E, Cattaneo G, Acosta R, Blümich B, et al. Desktop MRI as a promising tool for mapping intra-aneurismal flow. Magn Reson Imaging. 2015;33:328–35.
194. Lim V, Hobby A, McCarthy MJ, McCarthy KL. Laminar mixing of miscible fluids in a SMX mixer evaluated by magnetic resonance imaging (MRI). Chem Eng Sci. 2015;137:1024–33.

195. Mihailova O, Lim V, McCarthy MJ, McCarthy KL, Bakalis S. Laminar mixing in a SMX static mixer evaluated by positron emission particle tracking (PEPT) and magnetic resonance imaging (MRI). Chem Eng Sci. 2015;137:1014–23.
196. Adachi S, Ozeki T, Shigeki R, Handa S, Kose K, Haishi T, et al. Development of a compact magnetic resonance imaging system for a cold room. Rev Sci Instrum. 2009;80:054701.
197. Nakamura T, Tamada D, Yanagi Y, Itoh Y, Nemoto T, Utumi H, et al. Development of a superconducting bulk magnet for NMR and MRI. J Magn Reson. 2015;259:68–75.
198. Ogawa K, Nakamura T, Terada Y, Kose K, Haishi T. Development of a magnetic resonance microscope using a high T_c bulk superconducting magnet. Appl Phys Lett. 2011;98:234101.
199. Nordon A, McGill CA, Littlejohn D. Evaluation of low-field nuclear magnetic resonance spectrometry for at-line process analysis. Appl Spectrosc. 2002;56:75–82.
200. Dalitz F, Cudaj M, Maiwald M, Guthausen G. Process and reaction monitoring by low-field NMR spectroscopy. Prog Nucl Magn Reson Spectrosc. 2012;60:52–70.
201. Danieli E, Perlo J, Casanova F, Blümich B. High-performance shimming with permanent magnets. In: Codd SL, Seymour D, editors. Magnetic resonance microscopy. Weinheim: Wiley-VCH; 2009. p. 487–500.
202. Singh K, Blümich B. NMR spectroscopy with compact instruments. TrAC Trends Anal Chem. 2016. doi:10.1016/j.trac.2016.02.014.
203. Riegel SD, Leskowitz GM. Benchtop NMR spectrometers in academic teaching. TrAC Trends Anal Chem. 2016. doi:10.1016/j.trac.2016.01.001.
204. Elipe MVS, Milburn RR. Monitoring chemical reactions by low-field benchtop NMR at 45 MHz: pros and cons. Magn Reson Chem. 2016;54:437–43.
205. Küster SK, Casanova F, Danieli E, Blümich B. High-resolution NMR spectroscopy under the fume hood. Phys Chem Chem Phys. 2011;13:13172–6.
206. Zientek N, Laurain C, Meyer K, Kraume M, Guthausen G, Maiwald M. Simultaneous ^{19}F-^{1}H medium resolution NMR spectroscopy for online reaction monitoring. J Magn Reson. 2014;249:53–62.
207. Gouilleux B, Charrier B, Danieli E, Dumez J-N, Akoka S, Felpin FX, et al. Real-time reaction monitoringh by ultrafast 2D NMR on a benchtop spectrometer. Analyst. 2015;140:7854–8.
208. Gouilleux B, Charrier B, Akoka S, Felpin FX, Rodriguez-Zubiri M, Giraudeau P. Ultrafast 2D NMR on a benchtop spectrometer: applications and perspectives. TrAC Trends Anal Chem. 2016. doi:10.1016/j.trac.2016.01.014.
209. Meyr K, Kern S, Zientek N, Guthausen G, Mailwald M. Process control with compact NMR. TrAC Trends Anal Chem. 2016. doi:10.1016/j.trac.2016.03.016.
210. Garro-Linck Y, Killner M, Danieli E, Blümich B. Mobile low-field NMR spectroscopy for biodiesel analysis. Appl Magn Reson. 2013;44:41–53.
211. Killner MHM, Garro-Link Y, Danieli E, Rohwedder JJR, Blümich B. Compact NMR specroscopy for real-time monitoring of a biodiesel production. Fuel. 2014;130:240–7.
212. Obeidat SM. The use of ^{1}H NMR and PCA for quality assessment of gasoline of different octane number. Appl Magn Reson. 2015;46:875–83.
213. Guthausen G, Garnier A, Reimert R. Investigation of hydrogenation of toluene to methylcyclohexane in a trickle bed reactor by low-field nuclear magnetic resonance spectroscopy. Appl Spectrosc. 2009;63:1121–7.
214. Kreyenschulte D, Paciok E, Regestein L, Blümich B, Büchs J. Online monitoring of fermentation processes via non-invasive low-field NMR. Biotechnol Bioeng. 2015;112:810–21.
215. Vargas MA, Cudaj M, Hailu K, Sachsenheimer K, Guthausen G. Online low-field ^{1}H NMR spectroscopy: monitoring of emulsion polymerization of butyl acrylate. Macromolecules. 2010;43:5561–8.
216. Sans V, Porwool L, Dragone V, Cronin L. A self-optimizing synthetic organic reactor system using real-time in-line NMR spectroscopy. Chem Sci. 2015;6:1258–64.
217. Cudaj M, Guthausen G, Hofe T, Wilhelm M. SEC-MR-NMR: online coupling of size exclusion chromatography and medium resolution NMR spectroscopy. Macromol Rapid Commun. 2011;32:665–70.

218. Cudaj M, Guthausen G, Hofe T, Wilhelm M. Online coupling of size exclusion chromatography and low-field ^{1}H-NMR spectroscopy. Macromol Chem Phys. 2012;18:1933–42.
219. Sillerud LO, McDowell AF, Adolphi N, Serda RE, Adams DP, Vasile MJ, et al. ^{1}H NMR detection of superparamagnetic nanoparticles using a microcoil and novel tuning circuit. J Magn Reson. 2006;181:181–90.
220. Cistola DP, Robinson MD. Compact NMR relaxometry of relaxometry of human blood and blood components. TrAC Trends Anal Chem. 2016. doi:10.1016/j.trac.2016.04.020.
221. Luo Z-X, Fox L, Cummings M, Lowrey TJ, Daviso E. New forntiers in *in vitro* medical diagnostics by low field T_2 magnetic resonance relaxometry. TrAC Trends Anal Chem. 2016. doi:10.1016/j.trac.2016.02.025.
222. Haun JB, Castro CM, Wang R, Peterson VM, Marinelli BS, Lee H, et al. Micro-NMR for rapid molecular analysis of human tumor samples. Sci Transl Med. 2011;3:71ra16.
223. Shao H, Min C, Issadore D, Liong M, Yoon TY, Weissleder R, et al. Magnetic nanoparticles and micro NMR for diagnostic applications. Theranostics. 2012;2:55–65.
224. Min C, Shao H, Issadore D, Liong M, Weissleder R, Lee H. Diagnostic magnetic resonance technology. In: Issadore D, Westerveld RM, editors. Point-of care diagnostics on a chip. Heidelberg: Springer; 2013. p. 197–222.
225. Mylonakis E, Clancy CJ, Ostrosky-Zeichner L, Garey KW, Alangaden GJ, Vazquez J, et al. T2 magnetic resonance assay for the rapid diagnosis of candidemia in whole blood: a clinical trial. Clin Infect Dis. 2015;60:892–9.
226. Utz M, Landers J. Magnetic resonance and microfluidics. Science. 2010;330:1056–8.
227. Harel E. Lab-on-a-chip detection by magnetic resonance methods. Prog Nucl Magn Reson Spectrosc. 2010;57:293–305.
228. Finch G, Yilmaz A, Utz M. An optimized detector for in-situ high-resolution NMR in microfluidic devices. J Magn Reson. 2016;262:73–80.
229. Sun N, Yoon T-J, Lee H, Andress W, Weissleder R, Ham D. Palm NMR and 1-chip NMR. IEEE J Solid State Circ. 2011;46:342–52.
230. Sun N, Ham D. Handheld NMR systems for biomolecular sensing. In: Johns M, Fridjonsson EO, Vogt S, Haber A, editors. Mobile NMR and MRI. Cambridge: Royal Society of Chemistry; 2016. p. 158–82.
231. Sun N, Liu Y, Qin L, Lee H, Weissleder R, Ham D. Small NMR biomolecular sensors. Solid-State Electron. 2013;84:13–21.
232. Oligschläger D, Glöggler S, Watzlaw J, Brendel K, Jaschtschuk D, Colell J, et al. A miniaturized NMR-MOUSE with a high magnetic field gradient (Mini-MOUSE). Appl Magn Reson. 2015;46:181–202.
233. Pille C. Health and nutrition advisor. Bachelor thesis. Münster School of Design, Münster; 2014.
234. Blümich B, Paciok E. Outlook: Quo Vadis, NMR? In: Johns M, Fridjonson EO, Vogt S, Haber A, editors. Mobile NMR and MRI. Cambridge: Royal Society of Chemistry; 2016. p. 310–30.
235. Beckonert O, Keun HC, Ebbels TMD, Bundy J, Holmes E, Lindon JC, et al. Metabolic profiling, metabolomic and metabonomic procedures for NMR spectroscopy of urine, plasma, serum and tissue extracts. Nat Protoc. 2007;2:2692–703.
236. Larive CK, Barding GA, Dinges MM. NMR spectroscopy for metabolomics and metabolic profiling. Anal Chem. 2015;87:133–46.
237. Ravanbakhsh S, Liu P, Bjorndahl TC, Mandal R, Grant JR, Wilson M, et al. Accurate, fully-automated NMR spectral profiling for metabolomics. PLoS One. 2015;10:e0124219.
238. Wongravee K, Lloyd GR, Silwood CJ, Grootveld M, Brereton RG. Supervised self organizing maps for classification and determination of potentially discriminatory variables: illustrated by application to nuclear magnetic resonance metabolomic profiling. Anal Chem. 2010;82:628–38.
239. Luchinat C, Tenori L. Analysis of ^{1}H NMR metabolomics: from individual fingerprints to food analysis. In: Capozzi F, Laghi L, Belton PS, editors. Magnetic resonance in food science:

defining food by magnetic resonance. Cambridge: Royal Society of Chemistry; 2015. p. 190–200.
240. Halse ME. Perspectives for hyperpolarization in compact NMR. TrAC Trends Anal Chem. 2016. doi:10.1016/j.trac.2016.05.004.
241. Jeschke G, Frydman L, editors. Hyperpolarization NMR comes of age. A special Issue on the present and future of dynamic nuclear polarization. J Magn Reson. vol. 264. Amsterdam: Elsevier; 2016.
242. Acosta RH, Blümler P, Münnemann K, Spiess HW. Mixture and dissolution of laser polarized noble gases: spectroscopic and imaging applications. Prog Nucl Magn Reson Spectrosc. 2012;66:40–69.
243. Ardenkjaer-Larsen JH. On the present and future of dissolution-DNP. J Magn Reson. 2016;264:3–12.
244. Green RA, Adams RW, Duckett SB, Mewis RE, Williamson DC. The theory and practice of hyperpolarization in magnetic resonance using parahydrogen. Progr Magn Reson Spectrosc. 2012;67:1–48.
245. Wemmer DE. Hyperpolarized xenon biosensors and hyperCest. In: Meersmann T, Brunner E, editors. Hyperpolarized xenon-129 magnetic resonance: concpets, production, techniques and applications. Oxford: Royal Chemistry of Society; 2015. p. 249–60.
246. Jimenez-Martinez R, Kennedy DJ, Rosenbluth M, Donley EA, Knappe S, Seltzer SJ, et al. Optical hyperpolarization and NMR detection of ^{129}Xe on a microfluidic chip. Nat Commun. 2014;5:3908.
247. Parker AJ, Zia W, Rehorn CWG, Blümich B. Shimming Halbach magnets utilizing genetic algorithms to profit from material imperfections. J Magn Reson. 2016;265:83–9.
248. Danieli E, Blümich B, Zia, Leonards H. Method for a targeted shaping of the magnetic field of permanent magnets. WO 2015043684 A1 pending. published 2 Apr 2015.
249. Terada Y, Ishi K, Tamada D, Kose K. Power optimization of a planar single-channel shim coil for a permanent magnet circuit. Appl Phys Express. 2013;6:026701.
250. While PT, Korvink JG. Designing MR shim arrays with irregular coil geometry: theoretical considerations. IEEE Trans Biomed Eng. 2014;61:1614–20.
251. Ledbetter MP, Crawford CW, Pines A, Wemmer DE, Knappe S, Kitching J, et al. Optical detection of NMR J-spectra at zero magnetic field. J Magn Reson. 2009;199:25–9.
252. Savukov IM, Lee S-K, Romalis MV. Optical detection of liquid-state NMR. Nature. 2006;442:1021–4.
253. Meier RC, Höfflin J, Badility V, Wallrabe U, Korvink JG. Microfluidic integration of wirebonded microcoils for on-chip applications in nuclear magnetic resonance. J Micromech Microeng. 2014;24:045021.
254. Spengler N, Moazenzadeh A, Meier RC, Badilita V, Korvink JG, Wallrabe U. Micro-fabricated Helmholtz coil featuring disposable microfluidic sample inserts for applications in nuclear magnetic resonance. J Micromech Microeng. 2014;24:034004.
255. Spengler J, Höfflin J, Moazenzadeh A, Mager D, MacKinnon N, Badilita B, et al. Heternuclear micro-helmholtz coil facilitates μmrRange spatial and sub-hz spectral resolution NMR of nL-volume samples on customisable microfluidic chips. PLoS One. 2016;11:e0146384.
256. Suefke M, Liebisch A, Blümich B, Appelt S. External high-quality-factor resonator tunes up nuclear magnetic resonance. Nat Phys. 2015;11:767–71.
257. Anders J, Handwerker J, Ortmanns M, Boero G. A low-power high-sensitivity single-chip receiver for NMR microscopy. J Magn Reson. 2016;266:41–50.
258. Grisi M, Gualco G, Boero G. A broadband single-chip transceiver for multi-nuclear NMR probes. Rev Sci Instrum. 2015;86:044703.
259. Ha D, Paulsen J, Sun N, Song Y-Q, Ham D. Scalable NMR spectroscopy with semiconductor chips. Proc Natl Acad Sci. 2014;111:11955–60.